DEPARTAMENTO DE CIÊNCIAS DA VIDA

FACULDADE DE CIÊNCIAS E TECNOLOGIA
UNIVERSIDADE DE COIMBRA

Involvement of vascular dysfunction in the neurogenesis impairment that occurs in Alzheimer's disease

Dissertação apresentada à Universidade de Coimbra para cumprimento dos requisitos necessários à obtenção do grau de Mestre em Biologia Celular e Molecular, realizada sob a orientação científica da Professora Doutora Elisabete Baptista Ferreiro (Universidade de Coimbra) e da Professora Doutora Emília Duarte (Universidade de Coimbra).

Ana Raquel Martins Fontes

2014

Para os meus pais

Agradecimentos

A concretização desta etapa da minha vida não só é resultado de um esforço próprio mas também da colaboração, apoio e disponibilidade de muitas pessoas. Por isso, quero expressar o meu agradecimento a todas essas pessoas, sem as quais não teria sido possível a concretização desta fase importante da minha vida.

À doutora Elisabete Baptista Ferreiro, sobretudo pela orientação séria e meticulosa, mas igualmente por me ter dado a oportunidade de trabalhar na Ciência, transmitindo ensinamentos e experiências que, sem dúvida contribuíram para a minha aprendizagem ao longo deste percurso, assim como a construção dos meus interesses. Agradeço a disponibilidade dispensada, seriedade na condução dos trabalhos e, ainda a amizade com que sempre me distingui. A sua perserverância e entusiasmo não me farão esquecer de si.

Ao doutor Jorge Valero quero dedicar um agradecimento especial pela disponibilidade demonstrada e pela ajuda valiosa que foi capaz de prestar ao longo deste ano, sem a qual a realização deste trabalho não teria sido possível. O seu contributo no processamento de imagem e construção de macros foi determinante para a realização deste trabalho. Obrigada ainda pelos momentos de boa disposição. Como disse: “Sicence is fun”!

Ao grupo de investigação “Disfunção Mitocondrial e Sinalização em Neurodegeneração” por me terem acolhido.

Ao meu irmão Helder pelo carinho demonstrado e pelas palavras de incentivo.

À minha tia Celeste pelas palavras de ânimo e pelos conselhos que sempre me prestou.

Ao meu padrinho pelo apoio, interesse e preocupação demonstrados.

Aos meus amigos, Lila e João pela amizade que sempre demonstraram.

Ao Sr. Alberto e à Lisandra pela simpatia e por me fazerem sentir parte da família desde que me conheceram.

Aos meus pais, a quem devo a realização desta tese, quero manifestar o meu profundo reconhecimento pela confiança que sempre depositaram em mim, mostrando-me que não existe mérito sem trabalho. O vosso apoio incondicional foi determinante para mim. Sou-vos grata por todo o vosso contributo para a realização desta etapa, pela manifestação do vosso amor e por terem partilhado dos meus desejos e anseios. Por tudo o que vocês representam para mim, dedico-vos um obrigado muito especial.

Ao meu namorado Nelson, pelo companheirismo e pelo apoio constante concretizado pela enorme paciência que revelou nos momentos mais frágeis que passei e pelo carinho que sempre me transmitiu. Foi uma sorte ter-te conhecido, a tua presença na minha vida faz de mim uma pessoa mais confiante! Obrigada pela força que me transmitiste ao longo deste percurso, pelo interesse que demonstraste no meu trabalho. Pela tua dedicação, pelo momentos de mau humor que suportaste e também pelos muitos momentos de alegria que partilhámos expresso aqui o meu mais sincero agradecimento. Foi um prazer ter enfrentado este desafio contigo ao meu lado. Obrigada, meu amor!

À Universidade de Coimbra e ao Centro de Neurociências e Biologia Celular pelas instalações necessárias à realização deste trabalho.

À cidade da Coimbra que me acolheu e me encantou.

Table of contents

List of abbreviations 1

Resumo 4

Abstract.....6

Chapter 1 – Introduction.....7

1.1 Alzheimer's disease 8

1.1.1. Alzheimer's disease: an overview.....8

1.1.2. Pathophysiology and risk factors 10

1.1.3. Animal models of Alzheimer's disease: 3xTg-AD mouse model.....12

1.2. Cerebral vasculature and neurogenesis in Alzeimer's disease 14

1.2.1. Blood-brain barrier and the neurovascular unit.....14

1.2.2. Cerebrovascular alterations in Alzheimer's disease 16

1.3. Adult neurogenesis.....17

1.3.1. Neurogenesis in the adult hippocampal dentate gyrus and the vascular niche ...19

1.3.2. Altered hippocampal neurogenesis in Alzheimer's disease 21

Chapter 2 – Objectives 23

Chapter 3 – Materials & Methods 26

3.1. Animals and ethic statements 27

3.2. Experimental procedures 28

3.2.1. Vascular studies – Blood vessels characterization in DG.....28

3.2.1.1. Dextran administration and tissue processing 28

3.2.1.2. Evans blue administration and tissue processing.....28

3.2.2. Immunofluorescence staining 30

3.3. Data acquisition 31

3.3.1. Blood vessels 3D reconstruction 31

3.3.2. Blood vessels volume analysis in DG 32

3.3.3. Blood vessels complexity analysis in DG 33

3.3.4. Blood vessels functionality analysis in DG 34

3.3.5. Analysis of blood vessels integrity by leakage quantification in DG 35

3.3.6. Analysis of neural stem cells colocalization with vessels 35

3.4. Statistical analysis 36

Chapter 4 - Results 37

4.1. Microvasculature is affected in the DG of 3 month-old 3xTg-AD mice 38

4.1.1. Blood vessels volume is decreased in the SGZ of 3 month-old 3xTg-AD mice 38

4.1.2. Complexity of blood vessels is decreased in the DG of 3 month-old 3xTg-AD mice 40

4.1.3. Loss of blood vessels functionality in the DG of 3 month-old 3xTg-AD mice 43

4.1.4. Blood vessels integrity is affected in the DG of 3 month-old 3xTg-AD mice 46

4.1.5. Neural stem cells proximity to blood vessels is increased in 3 month-old 3xTg-AD mice 49

Chapter 5 - Discussion 52

Chapter 6 - Conclusion 57

Chapter 7 - References 59

List of Abbreviations

3xTg-AD	triple-transgenic mouse model of AD
AD	Alzheimer's disease
anti-PECAM	platelet-endothelial cell adhesion molecule antibody
ApoE4	allele 4 of apolipoprotein E gene
APP	amyloid precursor protein
APPSwe	swedish mutant amyloid precursor protein
As	astrocyte
Aβ	amyloid-β aggregates
BBB	blood-brain barrier
BDNF	brain-derived neurotrophic factor
BSA	bovine serum albumin
BV	blood vessel
CA1	*Cornu Ammonis* area 1 from hippocampus
CA2	*Cornu Ammonis* area 2 from hippocampus
CA3	*Cornu Ammonis* area 3 from hippocampus
CBF	cerebral blood flow
CECs	cerebral endothelial cells
CNS	central nervous system
CSF	cerebral spinal fluid
DCX	doublecortin
DG	dentate gyrus
EGF	epidermal growth factor
EU	*European Union*
FDG	fluorodeoxyglucose

FGF	fibroblast growth factor
FGF-2	fibroblast growth factor-2
FMUC	Faculdade de Medicina da Universidade de Coimbra
GCL	granule cell layer
GCs	granular cells
GDNF	glial cell-derived neurotrophic factor
GFAP	glial fibrillary acidic protein
i.p.	intraperitoneal
IGF-1	insulin growth factor-1
IgG	immunoglobulin G
IPC	intermediate progenitor cell
ML	molecular layer
MRI	magnetic Resonance Imaging
NB	neuroblast
NeuN	neuronal nuclear antigen
NFTs	intracellular neurofibrillary tangles
NGF	nerve growth factor
NMDA	*N*-metyl-D-aspartate
NonTg	non-transgenic
NSCs	neural stem cells
NVU	neurovascular unit
OB	olfactory bulb
OCT	optimum cutting temperature compound
PBS	phosphate-buffered saline
PET	positron emission tomography
PFA	paraformaldehyde

PSA-NCAM	polysialylated form of the neural cell adhesion molecule
PSEN1	presenilin 1
PSEN2	presenilin 2
RMS	rostral migratory stream
ROIs	regions of interest
SEM	standard error of the mean
SGZ	subgranular zone
SOX2	sex determining region Y (SRY)-box 2
SPECT	single photon emission cmputed tomography
SVZ	subventricular zone
TUJ1	β-tubulin III
USA	United States of America
VEGF	vascular endothelial growth factor
WT	wild type

Resumo

A doença de Alzheimer (DA) é uma doença neurodegenerativa associada ao envelhecimento e caracterizada por uma deterioração progressiva da memória e de outras funções cognitivas. As características neuropatológicas desta doença incluem perda sináptica e neuronal, acumulação extracelular de péptidos beta-amilóide (Aβ), nas placas amilóides, e agregação de tau hiperfosforilada formando emaranhados neurofibrilares intracelulares. Vários estudos sugerem que na DA a neurogénese no hipocampo está alterada, contribuindo para os défices cognitivos ligados à neurodegenerescência que ocorre nesta doença. A neurogénese adulta é um processo através do qual as células estaminais neurais (CENs) têm capacidade de gerar novos neurónios no cérebro mamífero pós-natal. A neurogénese ocorre em microambientes especializados chamados nichos neurogénicos, onde a vasculatura desempenha um papel importante no funcionamento das CENs. De acordo com descobertas recentes, na DA existe uma associação entre disfunção cerebrovascular, défice cognitivo e neurodegenerescência. Resultados anteriores do nosso grupo de investigação demonstram uma diminuição na neurogénese no giro dentado (GD) do hipocampo de ratinhos machos triplo transgénicos para a DA (3xTg-AD) com 3 meses de idade.

A nossa hipótese de trabalho considera que a disfunção vascular precoce na DA pode contribuir para a deterioração observada na neurogénese. Para investigar esta hipótese caracterizamos a vasculatura no GD de ratinhos 3xTg-AD com 3 meses de idade e analisámos a relação entre os vasos sanguíneos e as CENs. Os nossos resultados mostram um decréscimo no volume e na complexidade da vasculatura, dada pela redução no número de ramificações e junções ao longo dos vasos sanguíneos. Além disso, observámos a perda de funcionalidade e integridade dos vasos sanguíneos no GD. Finalmente, um aumento na proximidade de CENS aos vasos sanguíneos foi observado na camada molecular (CM) do GD. Todos os resultados obtidos suportam a ocorrência de alterações precoces na vasculatura do GD de ratinhos 3xTg-AD e a existência de uma estreita relação entre as CENs e os vasos sanguíneos na DA. Os dados apoiam um possível papel dos vasos sanguíneos na redução da neurogénese observada no modelo de ratinho da DA usado.

Estes resultados podem assim trazer novas perspetivas no que diz respeito ao envolvimento das alterações cerebrovasculares na redução da neurogénese que é observada na DA.

Palavras-chave: doença de Alzheimer, disfunção cerebrovascular, neurogénese, giro dentado, nicho neurogénico.

Abstract

Alzheimer's disease (AD) is an age-related neurodegenerative disease characterized by a progressive deterioration of memory and other cognitive functions. The neuropathological hallmarks of this disorder include synaptic and neuronal loss, extracellular accumulation of amyloid-beta (Aβ) peptide in amyloid plaques and aggregation of hyperphosphorylated tau forming intracellular neurofibrillary tangles. Several findings suggest that impaired hippocampal neurogenesis may contribute to AD-related cognitive deficits linked to neurodegeneration. Adult neurogenesis is a process through which neural stem cells (NSCs) have the capacity to generate new neurons in the post-natal mammalian brain. Adult neurogenesis occurs within specialized microenvironments called neurogenic niches where vasculature plays an important role in NSCs fate. According to recent findings, there is an association between cerebrovascular dysfunction, cognitive deficit and neurodegeneration in AD. Previous results from our lab support a decrease in the neurogenesis occurring in the hippocampal dentate gyrus (DG) of 3 month-old triple transgenic (3xTg-AD) male mice. Therefore, we hypothesize that early AD-related vascular dysfunction may account for the observed impairment in neurogenesis. To explore this, we further characterize the vasculature in the DG of 3 month-old 3xTg-AD mice and analyze the relationship between blood vessels and NSCs. Our results show a decrease in the volume and complexity of the vasculature, given by a reduction in the number of branches and junctions per length of blood vessels. In addition, loss of functionality and integrity of blood vessels was also observed in this region. Furthermore, an increase in the proximity of stem cells processes to blood vessels was found in the molecular layer (ML) of DG. Taken together, these results support the occurrence of early alterations in the vasculature of the DG of 3xTg-AD mice and a close relationship between NSCs and blood vessels, which may play a role in reduced neurogenesis observed in this AD mouse model. These findings may bring new perspectives in the involvement of cerebrovascular changes in the neurogenesis impairment that occurs in AD.

Keywords: Alzheimer's disease, cerebrovascular dysfunction, neurogenesis, dentate gyrus, neurogenic niche.

Chapter 1

Introduction

1.1. Alzheimer's disease

1.1.1. Alzheimer's disease: an overview

Alzheimer's disease (AD) is the most prevalent form of dementia in ageing population worldwide [1]. Dementia is the general term used to designate all brain diseases characterized by cognitive functions loss and that affects the ability to perform some daily activities http://www.alzheimers.org.uk/site/scripts/documents_info.php?documentID=133, accessed in July 10th 2014). In 2006, about 26 million cases of AD were identified worldwide and it is estimated to rise to over 100 million by 2050 [2]. Since the greatest risk factor for developing AD is age and considering that nowadays people are living longer, AD represents an important health problem with social and economic impact on society [3-4]. AD is a progressive disease, gradually increasing its severity over time and can be divided in three different stages: mild, moderate and severe (Figure 1.1). In the early stages of the disease, patients experience short-term memory lapses, have difficulties performing daily tasks and show some signs of anxiety and personality changes [5]. At the moderate stage, patients have more frequent memory lapses, showing problems in recognizing people and being unable to perform most common daily activities. During this stage, patients start having motor deterioration, perceptual and logical thinking problems and some may become easily aggressive. In the severe stage, loss of memory becomes prevalent and the person with AD gradually losses verbal language ability and motor control, becoming totally dependent on others (http://www.alzheimers.org.uk/site/scripts/documents_info.php?documentID=133, accessed in July 10th 2014). This stage ends with the person's death, usually from complications such as pneumonia. Life expectancy of AD patients is, in average, 8 years after clinical diagnosis, varying depending on the patient age [6].

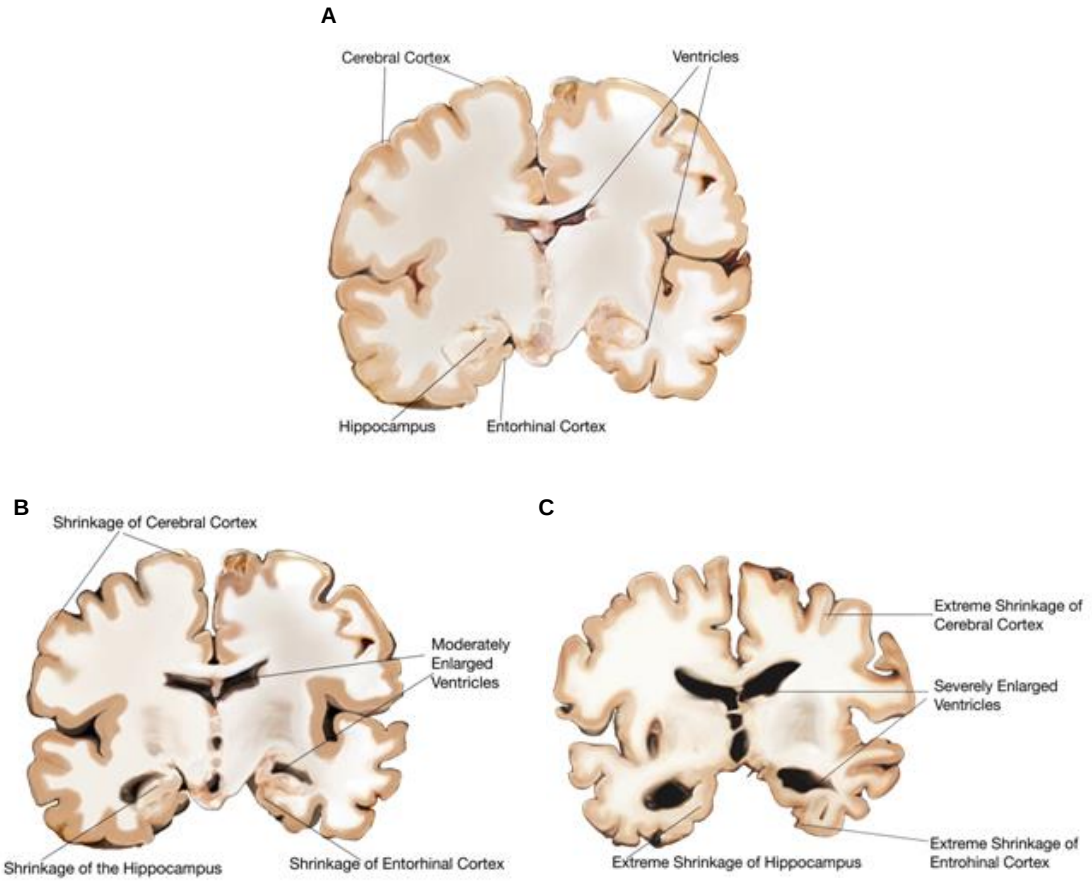

Figure 1.1.: Illustration of brain alterations in the different stages of AD: preclinical (A), mild to moderate (B) and severe (C) (adapted from http://www.nia.nih.gov/alzheimers/scientific-images).

Although AD diagnosis can only be confirmed through the identification of neuropathological hallmarks during patient's brain autopsy [7], a medical diagnosis can be performed based on life person's history, clinical observation, and cognitive evaluation. Imaging techniques have been very effective on complementing the overall AD diagnosis, namely positron emission tomography (PET) and single photon emission computed tomography (SPECT), used to assess brain function. These exams may show decreased cerebral metabolism and blood flow (Figure 1.2.). Structural brain scanning, obtained by magnetic resonance imaging (MRI), allows to examine hippocampus volume [8]. Currently, some biomarkers were identified in the cerebral spinal fluid (CSF) and are used to diagnose probable AD. Unfortunately, the existence of AD biomarkers in blood is still missing [9]. Despite these recent diagnostic techniques, an early specific diagnosis of AD would be essential for potential prevention of AD, since AD share similar symptoms with other types of dementia [9].

To date, there are no treatments able to completely prevent the progression of AD. However, there are two types of drugs currently used to ameliorate AD symptoms: acetylcolinesterase inhibitors and *N*-metyl-D-aspartate (NMDA) receptor antagonists [10]. Acetylcholinesterase inhibitors, comprising donepezil, rivastigmine and galantamine, are known to reduce acetylcholine degradation in the brain by inhibiting acetylcholinesterase enzyme activity and restoring synaptic levels of acetylcholine neurotransmitter in AD brains [11]. Another type of treatment action is the use of an NMDA receptor antagonist, memantine that blocks glutamate neurotransmitter action, thus protecting neurons from glutamate excitotoxicity [12].

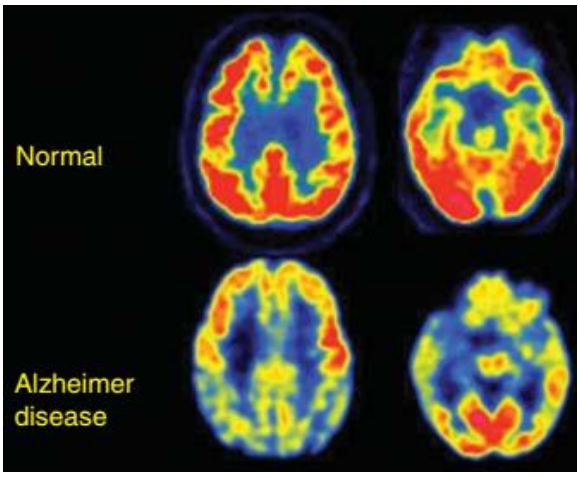

Figure 1.2.: Example of positron emission tomography (PET) images of cerebral metabolism with fluorodeoxyglucose (FDG-PET) of a normal control subject and a patient with mild AD. Yellow and blue represent cortical regions with severe hypometabolism brain regions. This pattern is well correlated with AD pathologic diagnosis (from [13]).

1.1.2. Pathophysiology and risk factors

AD can be divided into familial and sporadic forms [14]. Familial AD is due to autosomal dominant inheritance of mutations in amyloid precursor protein (APP), presenilin 1 (PS1) and presenilin 2 (PS2) genes. Familial forms of AD usually occurs before the age of 65 [15] and accounts for only 5% of AD cases [16]. The most common form of AD occurs sporadically, which fulfills the remaining 95% of AD cases [17], usually arises after the age of 65 [15] and has been related to age, gender, life style, vascular risk

factors (e.g. hypertension and diabetes), environmental factors (e.g. neurotoxins, pathogenic infections and head trauma) [18-19]. Also, the presence of allele 4 of apolipoprotein E (ApoE4) gene has been considered a risk factor for developing sporadic AD [20]. Regarding the neuropathology of AD, a progressive atrophy and gliosis is normally first identified in the hippocampus and medial temporal lobe and later associated to frontal and parietal lobes and finally to primary motor or sensory cortex (occipital lobe) (http://emedicine.medscape.com/ article/2003174-overview#aw2aab6b3), accessed in July 10th 2014. The neuropathological features of AD include the presence in the referred brain areas of extracellular plaques, denominated neuritic plaques, containing insoluble amyloid-β (Aβ) aggregates, and intracellular neurofibrillary tangles (NFTs) derived from an abnormal tau hyperphosphorylation (Figure 1.3. A) [21]. Aβ deposits can also be found around vessels or arteries, which accounts for amyloid angiopathy as another pathologic feature of AD (Figure 1.3. B) (http://emedicine.medscape.com/article/ 2003174-overview#aw2aab6b3, accessed in July 10th 2014). Disruption in glutamatergic and cholinergic neurotransmission are also observed in AD brains. All those characteristics eventually contribute to synaptic dysfunction and neuronal death that occurs in brain regions, mainly in cortex and hippocampus, essential for cognitive and memory functions [22]. Despite all neuropathological features currently described, the exact etiology of AD pathology is not completely known. Some hypotheses have been raised in order to explain the pathogenesis of this disorder, such as the amyloid hypothesis that describes that Aβ generated from the proteolytic cleavage of APP, triggers neurotoxic cascades leading to a widespread synaptic and neuronal disruption and dementia; tau hypothesis that considers that hyperphosphorylation of tau, a microtubule-associated protein, results in the formation of NFTs that interfere with cytoskeleton integrity and axonal transport leading to neuronal death [23]; cholinergic hypothesis that suggest that the depletion of cerebral levels of acetylcholine accounts for loss of cholinergic neurons contributing to cognitive impairment in AD [4]; glutamatergic hypothesis that indicates that an over-activation of extra-synaptic NMDA receptors due to increased glutamate results in excitotoxicity and neuronal death [24]; mitochondrial cascade hypothesis that claims that gene inheritance defines baseline mitochondrial function, and dysfunction of mitochondria overtime affects amyloid

precursor protein (APP) expression, APP processing, or Aβ accumulation [21]; vascular hypothesis that propose that vascular risk factors combined with aging contribute to a cerebral hypoperfusion and vascular endothelial impairment leading to neuronal metabolic death [25].

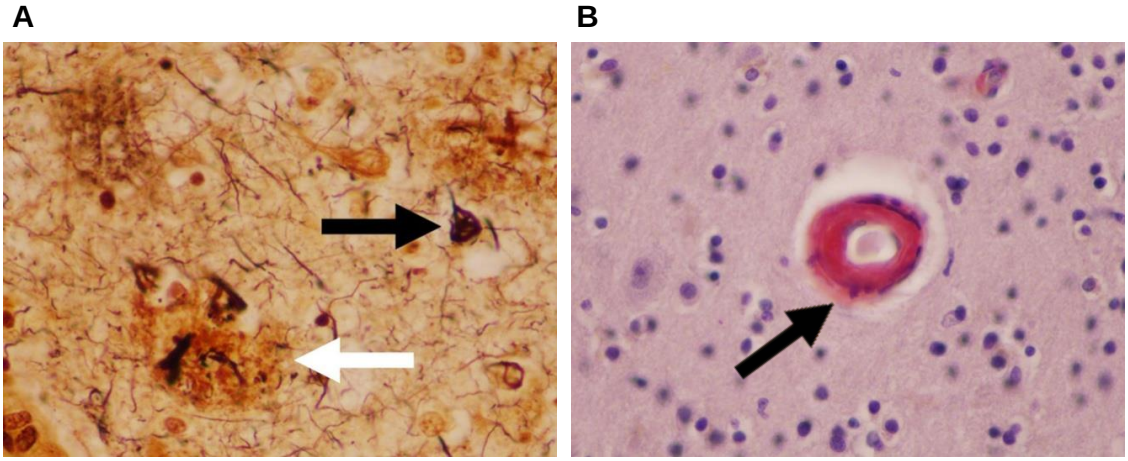

Figure 1.3.: (A) Neurofibrillary tangle (black arrow) and a neuritic plaque (white arrow) were identified by Bielschowsky silver staining in cortex at 400x magnification. (B) Small cortical artery at 400x magnification demonstrates Aβ deposition (black arrow) in the media of the vessel identified by Congo red staining technique (adapted from http://emedicine.medscape.com/article/2003174-overview#aw2aab6b3).

1.1.3. Animal models of Alzheimer's disease: 3xTg-AD mouse model

There are several transgenic animal models of AD used to study the etiology and therapeutic treatments of this neurodegenerative disease. Indeed, significant advances in the research of AD can be attributed to the use of these models [26].

The different mouse models used have been engineered by the introduction of transgenes linked to AD and mentioned above, with the purpose to represent the different pathological hallmarks of the disease. Among those, one has been created to better reproduce the entire AD spectrum, namely amyloid pathology, tau pathology, long-term potentiation (LTP) deficits and cognitive impairments that occurs in a time- and area-dependent form [27]. Indeed, the triple transgenic AD (3xTg-AD) mouse model is the unique transgenic model that expresses three human mutant genes: $PS1_{M146V}$, APP_{Swe}, and tau_{P301L} [27]. In this model, Aβ plaques appear first at 6 months of age in the neocortex and expand to the hippocampus at 12 months of age, whereas

NFTs appear afterwards [28]. Synaptic dysfunction and LTP deficits precede plaque and tangle formation and correlate with intraneuronal Aβ accumulation [27] that already occurs in 3-month old animals [29] (Figure 1.4.).

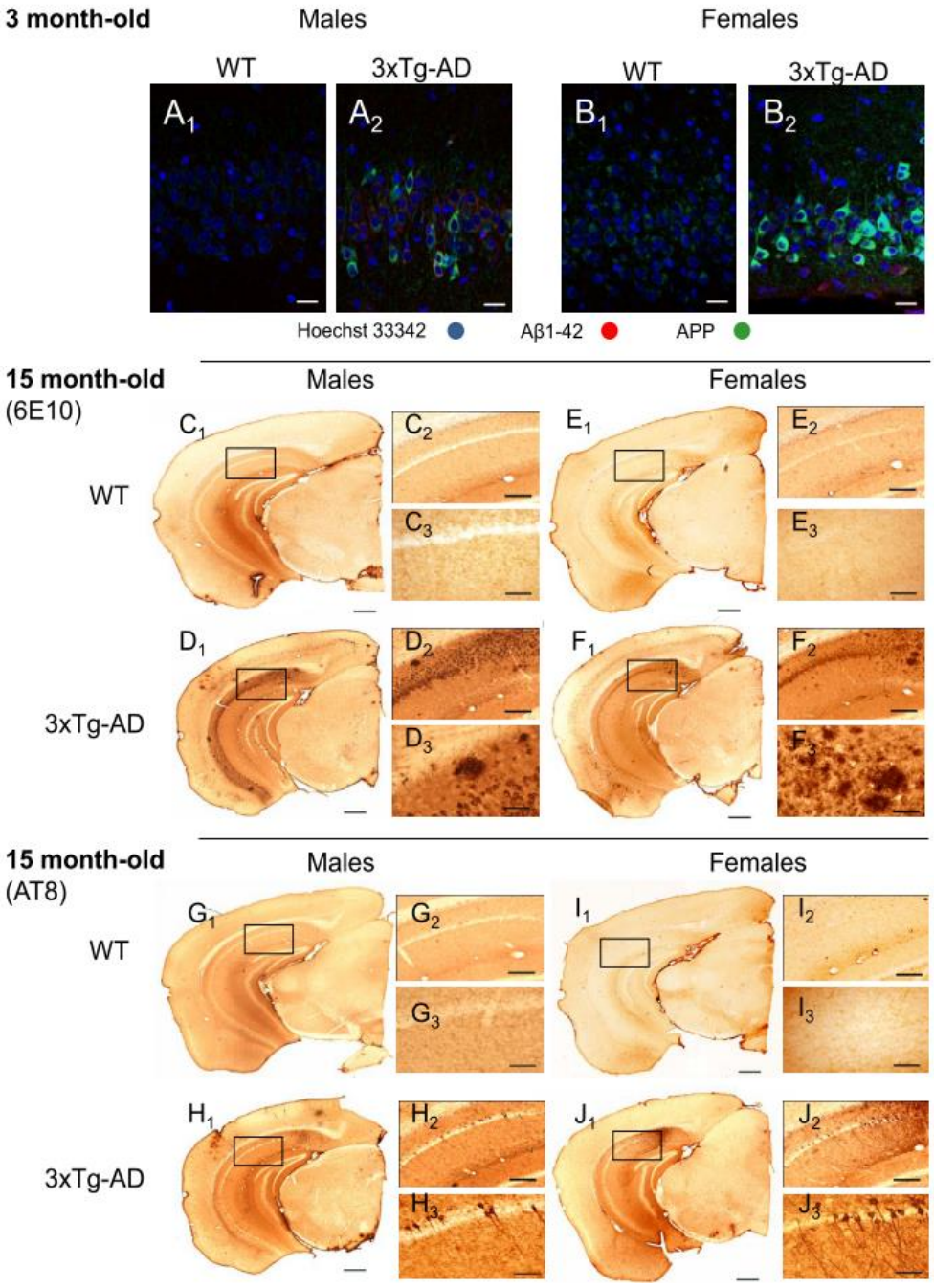

Figure 1.4.: Aβ deposition and hyperphosphorylated tau immunoreactivity in 3xTg-AD mice. In panels A and B, Aβ is immunostained with an antibody against Aβ1-42, while in panels C to F Aβ is immunostained with 6E10. Hyperphosphorylated tau was immunostained with AT8. A, B scale = 50 µm; C1-J1 scale = 500 µm; C2-J2 scale = 200 µm; C3-J3 scale = 50 µm (from [29]).

1.2. Cerebral vasculature and neurogenesis in Alzheimer's disease

AD research has been focused on amyloid plaques and NFTs hallmarks. However, the exact mechanism leading to neuronal cell death has not been yet elucidated. Recently, there has been an increasing interest in the potential vascular involvement in AD neurodegenerative process, since there are evidences showing cerebrovascular alterations in AD [30]. Furthermore, in the early stages of AD, it is believed that compromised neurogenesis arises before main pathological features or neuronal loss [31]. Since vasculature has a crucial role in adult neurogenesis, regulating the proliferation and differentiation of neural stem and progenitor cells, impairment of neurogenesis in AD might be associated with vascular dysfunction [32].

1.2.1. Blood-brain barrier and the neurovascular unit

Microenvironment control of the central nervous system (CNS) is essential for optimal neuronal function [33]. Blood brain barrier (BBB) is an important element in the control of molecular exchanges between blood and neural tissue [34]. The BBB is formed by tightly bounded cerebral endothelial cells (CECs) that form the cerebral microvessels of the CNS [34-35]. CECs are surrounded by astrocytes, pericytes, microglia and neurons forming a highly multicellular and coordinated system named neurovascular unit (NVU) (Figure 1.5.), that regulates the cerebral microvascular permeability [34, 36]. The CECs are different from peripheral endothelial cells having a superior number of mitochondria which results in a high metabolic activity [37]. The adhesion of CECs to each other is made by adherens junctions and tight junctions. These junction proteins are important for tissue integrity and vascular permeability [38], and the loss or disruption of these binding proteins compromises the integrity and functionality of the BBB, resulting in its breakdown [36].

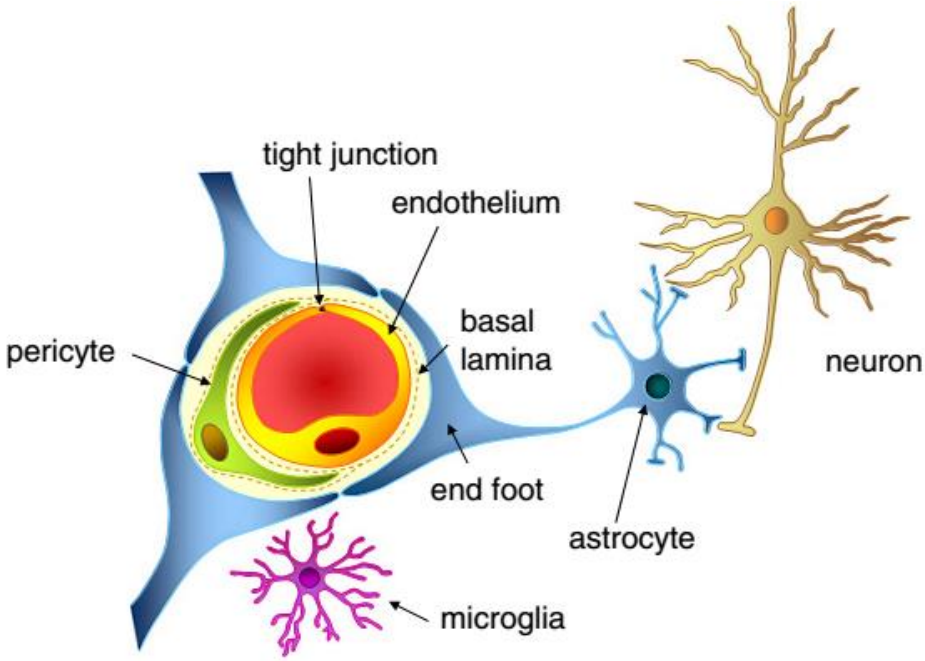

Figure 1.5.: Schematic representation of the neurovascular unit (from [33]). Endothelial cells linked through tight junctions form the BBB and are surrounded by pericytes, astrocytes, microglia and neurons, forming together the neurovascular unit responsible to maintain the normal brain functioning.

In the BBB, gaseous molecules and small lipophilic compounds can pass through the cellular membranes of CECs by passive diffusion. In turn, nutrients are transported by solute-carrier transporters, while large molecules cross the BBB by receptor-mediated transcytosis and cationized molecules by adsorptive-mediated transcytosis [34].

In the neurovascular unit, astrocytes and Pericytes interact closely with CECs in the maintenance of BBB function. Astrocytes end-feet cover a large part of the surface of CECs and are important in the control of the cerebral blood flow, provision of nutrients to the nervous tissue and repair the brain following traumatic injuries. Pericytes, separated from CECs by the basal lamina, are responsible for maintenance of vessels, angiogenesis and regulation of vascular permeability [39].

Blood vessel and nervous systems are formed together during embryonic development and therefore exert mutual influence. Endothelial and neuronal cells produce growth factors and their receptors as sensors for environmental alterations. The growth factors are responsible for endothelial and neuronal cells proliferation, migration and differentiation [40]. Vascular endothelial growth factor (VEGF), insulin growth factor-1

(IGF-1) and fibroblast growth factor (FGF) are some examples of angiogenic growth factors that induce endothelial cell survival, proliferation and differentiation as well as neurogenesis and neuroprotection. Nerve growth factor (NGF), brain-derived neurotrophic factor (BDNF) and glial cell-derived neurotrophic factor (GDNF), are some examples of neurogenic growth factors that promote neuronal survival, differentiation and protection, as well as angiogenesis and regulate BBB formation [40-41] .

In certain situations the temporary osmotic opening of the BBB is performed, such as in patients with brain tumor to improve the delivery of chemotherapy into the brain [42-43]. The temporary osmotic opening of the BBB can be performed using osmotic agents, such as mannitol, an hyperosmolar agent that is used, for example, to lower intracranial pressure in the brain after trauma [44] or to temporary open the BBB to allow the passage of albumin bound to tracers, such as the Evans blue dye [45] . Under normal physiologic conditions endothelium cells of the BBB are impermeable to albumin, leading to the retention of Evans blue dye bounded to albumin. When BBB is disrupted, endothelial cells loose their binding proteins allowing vascular leakage of Evans blue dye from blood vessels [46]. Mannitol opens the BBB through vasodilatation and cerebrovascular CECs shrinkage, causing the enlargement of the endothelial tight junctions and allowing Evans blue dye extravasation [42, 47].

1.2.2. Cerebrovascular alterations in Alzheimer's disease

It has been proposed that sporadic AD is initiated by vascular-related causes preceding the neurodegenerative process [48-49]. The following facts indicate an association between cerebrovascular dysfunction and AD pathogenesis: risk factors for AD, such as hypertension, diabetes mellitus, and atherosclerosis are related to vascular disorders [30]; therapies used to reduce AD progression also improves cerebral perfusion; regional brain microvascular alterations arise before cognitive and neuronal degeneration [50]; decreased cerebral blood flow (CBF) was detected early in AD through magnetic resonance imaging (MRI), transcranial doppler measurements, and single photon excitation computed tomography (SPECT) [51].

Numerous cerebrovascular morphological changes, such as decreased microvascular

density, increased number of fragmented vessels with damaged branches, increased capillary surface abnormalities, altered vessel diameter have been identified in AD [52]. Moreover, degeneration of endothelium identified by a reduction in CD34 and CD31 endothelial markers staining was observed in AD [53]. As a consequence of BBB disruption, the normal transport across the BBB is compromised, affecting the supply of essential metabolites such as O_2, amino acids and glucose, and thus the normal neuronal functioning [51].

Thereby, it is considered that neurovascular dysfunction is a key factor in AD development [54]. And so, the vascular system could be considered an alternative target for AD treatment.

1.3. Adult neurogenesis

In the past, it was believed that neurogenesis, a process of generating new functional neurons from precursors, occurred exclusively during embryonic and early postnatal development [55]. Santiago Ramón y Cajal, one of the first neuroanatomist, considered the adult nervous system immutable and not able to regenerate [56]. Later, Joseph Altman performed several studies that revealed the presence of newly generated neurons in specific regions of adult rat brain [57]. Since then, many studies have demonstrated the existence of neurogenesis in the adult mammalian brain. Currently, it is widely recognized that adult neurogenesis occurs from self-renewing and multipotent neural stem cells (NSCs) that reside mainly in two neurogenic regions of the mammalian central nervous system, the subventricular zone (SVZ) lining the lateral walls of the lateral ventricles and the subgranular zone (SGZ) of the hippocampal DG (Figure 1.6.) [58-59]. Progenitor cells from the SVZ migrate a long distance towards the olfactory bulb (OB) via the rostral migratory stream (RMS) [60], whereas neuronal progenitors in the SGZ migrate into the granule cell layer (GCL) [61]. In both regions, OB and DG, only a fraction of these newly-generated cells survive to complete their differentiation into functional mature local interneurons or granular cells (GCs), respectively [62].

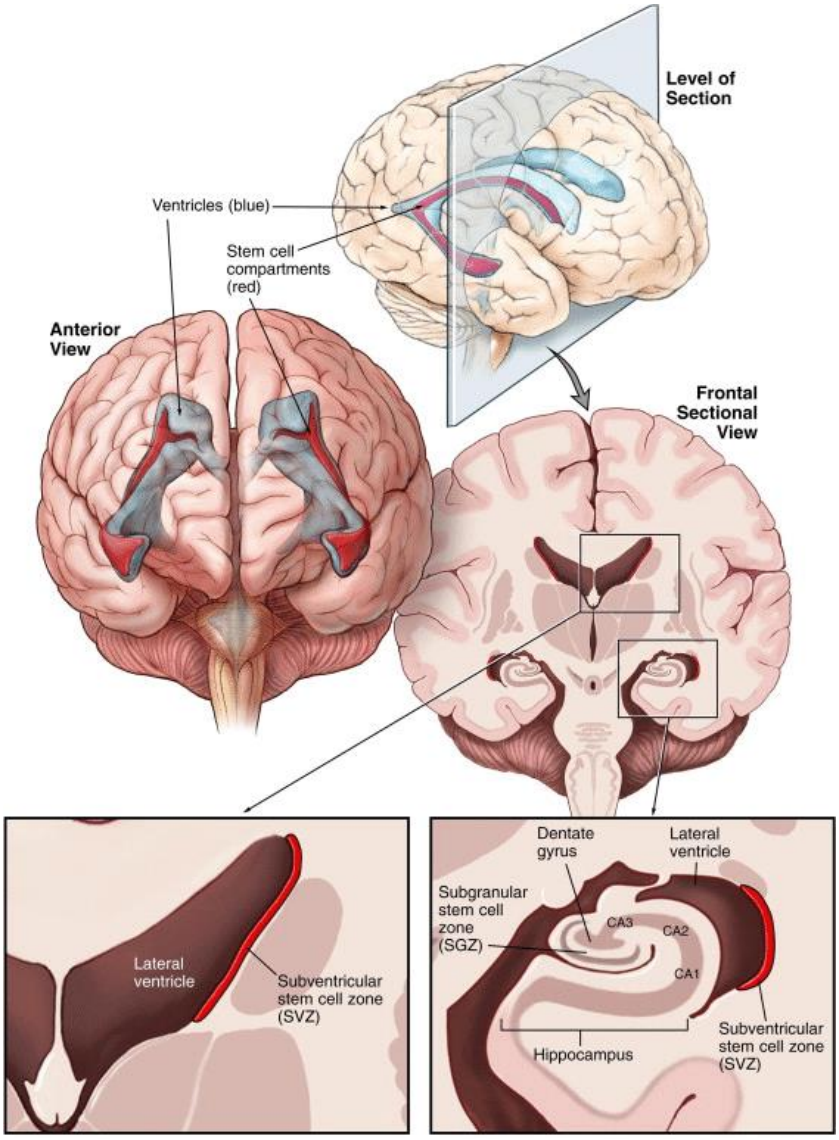

Figure 1.6.: Representation of the neurogenic regions in the adult human brain. Cortical brain section showing the subgranular zone (SGZ) of the hippocampal dentate gyrus, and the subventricular zone (SVZ) located at the lateral walls of the lateral ventricles. CA1, CA2, CA3 are regions of the hippocampus (from http://aboutcancer.com/brain_stem_cell_507.gif).

1.3.1. Neurogenesis in the adult hippocampal dentate gyrus and the vascular niche

In the SGZ of the adult hippocampal dentate gyrus, NSCs (also designated radial type-1 cells) give rise to intermediate progenitor cells (nonradial type-2a cells) that express stem/progenitor markers including the intermediate filament protein Nestin, the transcription factor Sox2 and glial fibrillary acidic protein (GFAP) [61]. These cells, in turn, produce Type-2b cells expressing the microtubule-associated protein doublecortin (DCX). These cells originate immature newborn granule cells or neuroblasts (type-3 cells) which migrate to the GCL and differentiate into mature GCs expressing NeuN or calbindin (Figure 1.7.) [61]. Although the relevance of new neurons is not totally clear [63], many evidences have revealed that they play a significant role in learning and memory functions [64].

Neurogenesis occurs within specialized microenvironments called neurogenic niches (Figure 1.8.), mainly formed by neural stem/progenitor cells, mature neurons, glia and endothelial cells that together modulate neurogenesis [66]. The importance of a microenvironment in the regulation of neurogenesis was raised from the observation that precursor cells isolated from neurogenic areas and transplanted into non-neurogenic regions showed low differentiation capacity [67]. In the adult SGZ neurogenic niche, the vasculature is a key element, since neural stem cells are located around blood vessels and neural progenitor cells proliferate together with endothelial precursors (angioblasts), in a close association with the microvasculature [32]. The observation that neurogenesis occurs related to a dynamic process of vascular recruitment suggests that there are signals that can simultaneously act on neural and endothelial precursors or, alternatively, that neurogenesis may be dependent on angiogenesis [68]. The meaningful of this vascular recruitment in SGZ can be related with the metabolic demand of neural proliferating cells. Moreover, the fact that neurogenesis occurs exclusively within such particular niche, where neural and endothelial precursors are tightly associated, indicates that vasculature may provide essential signals to induce neuronal determination [69].

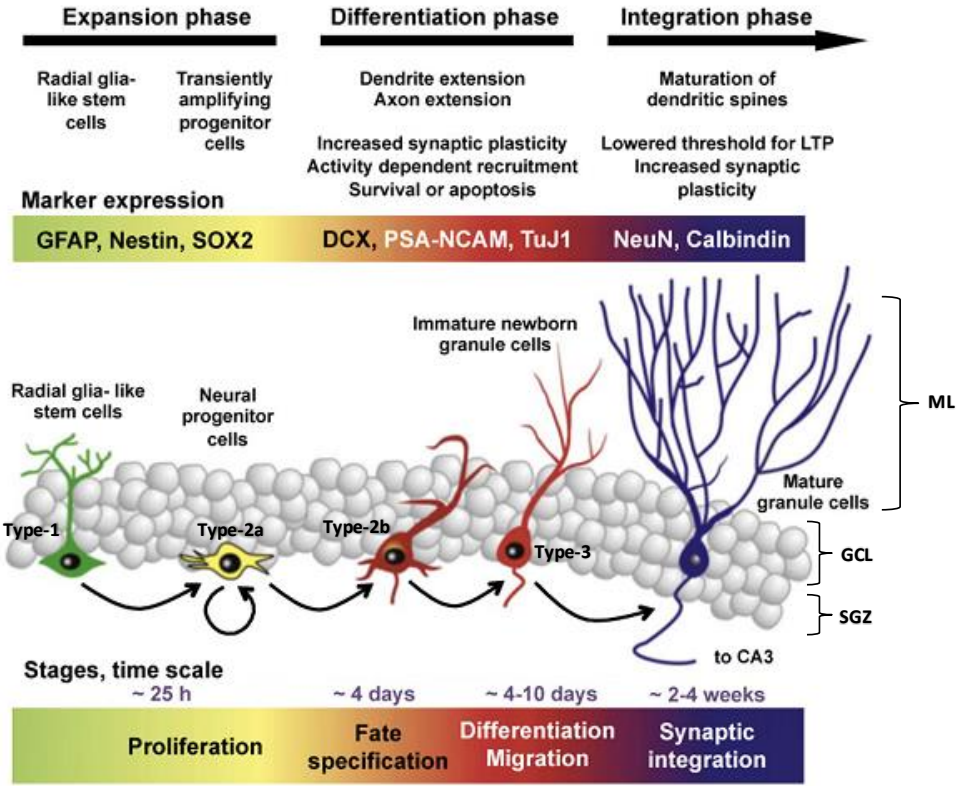

Figure 1.7.: Schematic representation of neurogenesis in the adult hippocampal dentate gyrus (adapted from [65]). Neurogenesis occurs in different stages: Radial glia-like stem cells (type-1 cells) in the subgranular zone (SGZ) divide and give rise to neural progenitor cells (type-2a and 2b cells). Then, type-2b cells differentiate into immature newborn granule cells or neuroblasts (type-3 cells), which migrate through the granule cell layer (GCL) and differentiate into mature granule cells that project their dendrites into the molecular layer (ML) and extend their axons towards the CA3 region of the hippocampus. GFAP: glial fibrillary acidic protein; Nestin: intermediate filament protein in nerve cells; SOX2: sex determining region Y (SRY)-box 2; DCX: doublecortin; PSA-NCAM: polysialylated form of the neural cell adhesion molecule; TuJ1: β-tubulin III; NeuN: neuronal nuclear antigen; Calbindin: Ca^{2+}-binding protein.

Several evidences point to a potential vascular involvement in neurogenesis. Numerous recent studies have contributed to demonstrate the vascular regulation of all adult neurogenesis stages [70]. It was shown that endothelial cells secrete brain-derived neurotrophic factor (BDNF) (involved in growth and differentiation of new neurons) and that, in coculture assay, they were able to induce self-renewal, as well as differentiation of neuronal precursors isolated from adult SVZ [71]. Furthermore, basic fibroblast growth factor (FGF-2), an angiogenic factor secreted by endothelial cells, is able to promote neural stem proliferation in vitro [72]. Some conditions known to

increase neurogenesis are also implicated in an increased production of angiogenic factors. For instance, vascular endothelial growth factor (VEGF), FGF-2, and epidermal growth factor (EGF) are up-regulated in brain regions affected by an ischemic lesion [73]. Moreover, circulating insulin-like growth factor-1 (IGF-1) has been shown to increase hippocampal neurogenesis induced by exercise [74].

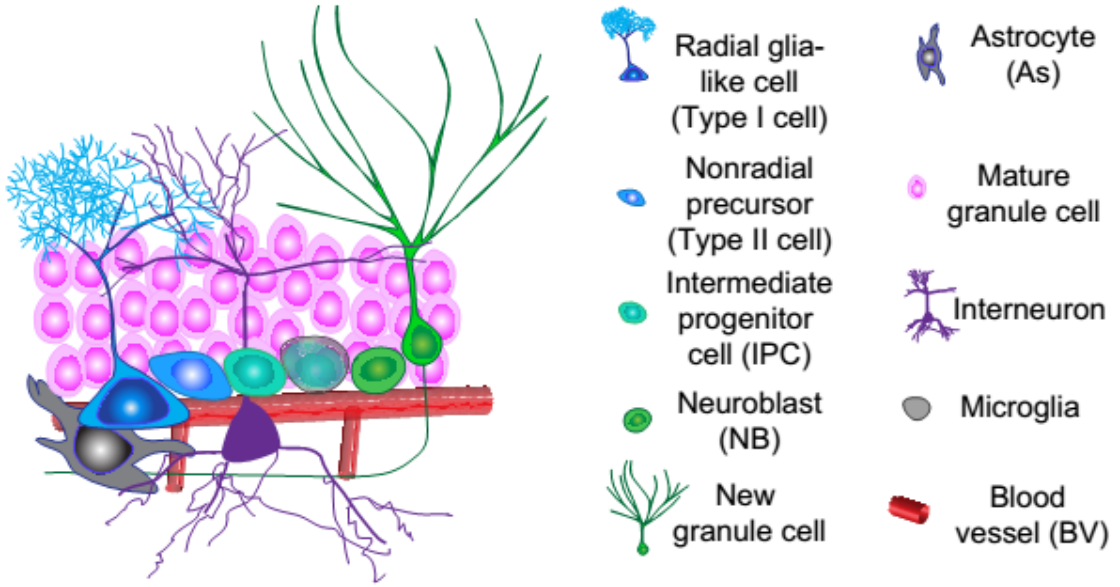

Figure 1.8.: A schematic representation of the neural stem cell niche in the SGZ in the DG of the hippocampus (adapted from [64]).

1.3.2. Altered hippocampal neurogenesis in Alzheimer's disease

Given the functional involvement of adult hippocampal neurogenesis in memory and learning functions, altered neurogenesis is proposed to contribute to early deterioration of hippocampal function in AD [31]. There has been a growing interest to understand whether and how neurogenesis is altered in AD and how these alterations can be related with the disease progression [75]. Over the past few years, various studies in human and animal models exhibiting some features of AD pathology support the evidence of alterations in neurogenesis [76-77]. However, there has been some controversy regarding the results obtained. Some studies present a decrease in neurogenesis, while others show increased neuronal production. As an example, Jin, et

al. (2004), reported increased neurogenesis in AD hippocampus in human brain tissue, however, Li, et al. (2008) have demonstrated for the first time that the newly generated neurons in the hippocampus are not able to differentiate into mature neurons [78-79]. Contrary to the findings of Jin, et al. (2004), studies conducted by Ziabreva et al., (2006) have demonstrated a reduction of neural progenitors in the SVZ of human brain tissues, suggesting that AD can impact differently the two main neurogenic regions [80]. Additionally, a recent study carried by Perry et al., (2012) showed a reduction in NSCs, an increase in the proliferation and no alterations in the number of neuroblasts and new differentiated neurons, concluding that alterations in neurogenesis may vary depending on the phases and areas of neurogenesis, as well as stages of AD [81].

Contradictory results obtained with animal mouse model of AD do not bring more light to this issue. In fact, a study performed by Chen et al. (2008) using a mouse model of AD-like neurodegeneration showed that neurogenesis was increased in the DG at early stages of neurodegeneration, while at late stages of degeneration the survival of newly generated neurons was impaired. These changes in neurogenesis were associated with the neuronal loss in the hippocampus, suggesting that neurogenesis may function as a brain repair mechanism to replace neuronal loss [82]. Another study using the 3xTg-AD mice showed a decreased proliferation in the hippocampus associated with the presence of Aβ plaques [83]. Moreover, Aβ accumulation triggers an inflammatory response that eventually contributes to affect neurogenesis [84]. However, a study performed in APP_{Swe}/PS1ΔE9 transgenic AD mouse model showed that impairments in neurogenesis occur prior to Aβ deposition and that may contribute to the early symptoms of AD. Therefore, it has been suggested that impairments in neurogenesis in the adult brain may underlie, in some degree, the cognitive deterioration and memory loss, contributing to the disease progression [85]. Furthermore, Jin et al. (2006) demonstrated that drugs used to treat cognitive impairment in AD, including AChE inhibitors and NMDA receptor antagonists, increase neurogenesis either in SGZ and SVZ [86].

All together, these findings suggest an important contribution of neurogenesis dysregulation in AD-related cognitive impairment. Thus, neurogenesis stimulation could be a potential therapeutic strategy in order to replace neurons that are lost during the disease and, thus, improve cognitive deficits [82, 87].

Chapter 2

Objectives

Recent studies have shown that cerebrovascular dysfunction may contribute to cognitive decline in AD and, thus, it is considered to play a major role in the pathogenesis of this neurodegenerative disease. Another important factor that contributes to early deterioration of cognitive function in AD can be the impairment of neurogenesis in hippocampus, a brain region affected in this disease. Considering the importance of cerebrovasculature in the neurogenic niche where new neurons are formed, the present work is based on the hypothesis that cerebrovascular dysfunction in DG may contribute to adult neurogenesis impairment in AD. Unpublished data from our group have shown impairment in neurogenesis in DG of 3 month-old 3xTg-AD male mice, observed by a decreased number of Sox2-positive stem cells and DCX-positive neural progenitor cells. Moreover, at this age, 3xTg-AD mice have soluble Aβ in neurons of the hippocampus and cortex and do not exhibit yet extracellular amyloid plaques deposition, neither tangles formation. Thus, these are important considerations for the results interpretation, in the sense that possible microvascular changes that could arise in the hippocampus early in the disease are independent of amyloid plaques and tangles formation. For these reasons, to investigate the proposed hypothesis, we decided to study whether alterations in the structure, integrity and functionality of the microvasculature occur in the hippocampal DG and how these alterations can affect neurogenesis in the DG of 3 month-old 3xTg-AD male mice.

The specific objectives of this work were:

- To characterize microvasculature in the SGZ, GCL and ML of the DG in the 3xTg-AD mouse model, by measuring :
  - blood vessels volume normalized to the volume of each corresponding DG region;
  - blood vessels branches normalized to the blood vessels length;
  - blood vessels junctions normalized to the blood vessels length;

- To evaluate the functionality of blood vessels in the SGZ, GCL and ML of the DG in the 3xTg-AD mouse model, by determining the percentage of colocalization between functional vessels and the totality of vessels ;

- To assess to blood vessels integrity in the SGZ, GCL and ML of the DG in the 3xTg-AD mouse model by measuring evans blue dye intensity ratio outside/inside blood vessels;

- To investigate the relationship between the blood vessels and NSCs in the DG, by measuring the proximity of these two elements of this neurogenic niche.

Investigating the relationship between cerebrovasculature and the generation and maturation of new neurons in the DG of the hippocampus can elucidate the involvement of blood vessels in neurogenesis impairment, and, thus, contribute to outline novel therapeutic strategies for AD.

Chapter 3

Materials & Methods

3.1. Animals and ethic statements

13 3xTg-AD (Figure 3.1.) and 17 control 3 month-old male mice were kept in the same room in cages enriched with a malleable paper bag, under controlled light (12 h light/dark cycle)) and temperature (23 ± 2°C) with free access to water and food. The breeding pairs of the homozygous 3xTg-AD and NonTg mice (C57BL6/129S background) were a generous gift from Dr. Frank Laferla, (University of California, Irvine) and were bred and maintained at our animal colony at the Center of Neuroscience and Cell Biology - Faculty of Medicine animal house. The 3xTg-AD mice were generated by injecting two transgenes, carrying respectively the APPSwe and the tauP30IL mutations, both under the control of mouse Thy1.2, in single-cell embryos of mutant homozygous PS1M146V knockin mice [27]. Animal experimental procedures were performed in accordance with institutional animal house, national (Bioterio FMUC; License nº 520.000.000.2006 from the Portuguese animal welfare authorities) and European Community (2010/63/EU) guidelines. The experiments were carried out in order to minimize the number of animals used and exposure to stress and suffering. The animals were sacrificed under anesthesia with 70 mg/Kg of pentobarbital.

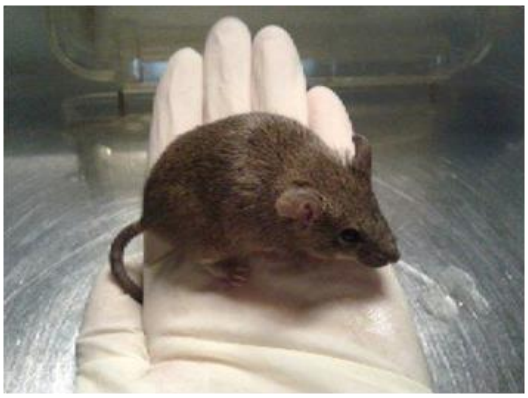

Figure 3.1.: Photo of a 3 month-old male triple-transgenic AD model (3xTg-AD) mouse (courtesy of Elisabete Ferreiro, from Centre for Neuroscience and Cell Biology, University of Coimbra).

3.2. Experimental procedures

3.2.1. Vascular studies – Blood vessels characterization in DG

3.2.1.1. Dextran administration and tissue processing

To label functional blood vessels, dextran Texas-Red 70 kDa (0.1 mL of a 10 mg/mL stock prepared in 0.9% NaCl solution; #D1844, Life Technologies, Paisley, UK) was injected into the left heart ventricle of anesthetized mice (n=4). After 5 min of the injection, brains were dissected out and placed in 4% (w/v) paraformaldehyde (PFA) (prepared in 0.1 M phosphate buffer; Sigma-Aldrich; St. Louis, Missouri, USA) for 3 overnights. Brains were then kept in phosphate buffered saline (PBS; containing 137 mM NaCl, 2.7 mM KCl, 10 mM Na_2HPO_4, 1.8 mM KH_2PO_4, pH 7.4) to remove the excess of PFA and were immersed in warm (~40 ºC) agar 4% (w/v) (prepared in distilled water) and then cooled down at 4 ºC. Right brain hemisferes were sectionated in 50 µm sagital slices using a vibratome (VIBRATOME® 1000 PLUS). Then, brain slices were processed for immunofluorescence staining.

3.2.1.2. Evans blue administration and tissue processing

Evans blue (molecular weight 961 Da) is a dye that binds to albumin in blood circulation, giving rise to a high-molecular complex (≈68 KDa), being retained within blood vessels under physiological conditions. When blood vessels integrity is compromised, Evans blue leaks out of the vessels, serving as an in vivo marker of blood vessels leakage.

A solution of Evans blue (0.1 mL of a 2 % (w/v) stock prepared in a 0.9 % NaCl solution (w/v); Sigma-Aldrich) was injected into the left heart ventricle of anesthetized mice (n=3 3xTg-AD; n=6 NonTg). Brains were dissected out after 5 min of the Evans blue injection. A NonTg mouse injected with 0.1 mL of a solution of 0.9 % NaCl (w/v), whithout Evans blue, was used as negative control. As positive control of blood vessels leakage, osmotic opening of the blood-brain barrier (BBB) was induced by injecting

intracardiacally a solution of mannitol [88] NonTg mice (n=1) were injected with Evans blue as described above, followed by the injection of mannitol (1.5 g/Kg body mass (w/w) from a solution of 25% (w/v) prepared in H_20 miliQ; Sigma-Aldrich) during 5 min, which is the maximal duration of the BBB opening using that hyperosmolar agent.

After decapitation, brains were quickly removed and fixed by immersion in PFA for 24 h, at 4 °C. For crioprotection, brains were immersed in a 30% sucrose solution (prepared in PBS Fisher), during 24h, at 4ºC. Brain hemispheres were then quickly frozen and stored at -80 °C. On the following day, frozen right hemisferes were embedded in Tissue-Tek® optimum cutting temperature (OCT) compound (Sakura) and cut into 50 µm thick saggital sections using a cryostat (Leica Microsystems CM3050 S, Germany), at −20 °C. The next day, slices were rinsed 3 x 5 min in PBS to remove OCT and incubated with Hoechst 33342 (dilution 1:10000 from a stock of 2 µg/mL, Molecular Probes®, Life Technologies) for nuclear labeling and 0.2 % Triton X-100 (v/v) (Thermo Fisher Scientific), preprared in PBS, for 30 min, at RT. After this, brain slices were rinsed in PBS (3 x 5 min), mounted on microscope gelatinized slides with antifading medium (Fluoroshield mounting medium, ab104135, Abcam). The next day, images of Evans blue staining in the hippocampal DG were acquired using a confocal LSM 510 Meta microscope (Carl Zeiss, Göttingen, Germany).

To avoid Evans blue degradation, brains were maintained in the dark during the protocol.

3.2.2. Immunofluorescence staining

Brain slices were rinsed 3 x 10 min in PBS, pH 7.4, and next immersed in blocking solution composed of 3 % (w/v) Bovine Serum Albumin (BSA) and 0.2 % Triton X-100 (v/v) in PBS, pH 7.4, for 1 h, at RT, with agitation. Brain slices were then incubated 3 overnights with primary antibodies prepared in the blocking solution, as listed in table 1, at 4 °C, with agitation. After this incubation period, tissue slices were rinsed in PBS, pH 7.4 (3 x 10min) and, then incubated with the appropriate secondary antibodies, as listed in table 1, and Hoechst 33342 (1:10000; Life Technologies, Paisley, UK), prepared in PBS pH 7.4 supplemented with 0.3 % BSA and 0.2 % Triton X-100, for 1h, at RT, with agitation. Finally, tissue slices were mounted on gelatinized glass slides with antifading medium (Fluoroshield Mounting Medium, ab104135, Abcam). The day after, image stacks of the hippocampal DG were acquired using a confocal LSM 510 Meta microscope.

Table 1: List of primary and secondary antibodies used for Immunohistochemistry

Primary antibodies	**Reference**	**Origin**	**Dilution**
Rat anti-PECAM-1*	550274	BD Pharmingen	1:100
Mouse anti-Nestin	MAB353	Millipore, Billerica, MA, USA	1:500
Goat anti-Sox2	sc-17320	Santa Cruz Biotechnology, Santa Cruz, CA, USA	1:1000
Secondary antibodies		**Origin**	**Dilution**
Donkey anti-rat Alexa Fluor 488	A-11006	Life Technologies, Paisley, UK	1:200
Donkey anti-mouse Alexa Fluor 594	A-11062	Life Technologies, Paisley, UK	1:1000
Donkey anti-goat Alexa Fluor 633	A-21082	Life Technologies, Paisley, UK	1:1000

* blocking with 3 % (w/v) BSA and 1 % Triton X-100 (v/v) in PBS, pH 7.4, for 1h

3.3. Data acquisition

3.2.1. Blood vessels 3D reconstruction

For the analysis of blood vessels volume, structure and functionality in DG, 94 confocal images with 4 stacks of 1.7 µm each (45 for 3xTg-AD and 49 for NonTg) of blood vessels (PECAM and dextran staining) and nuclei (Hoechst 33342 staining), were obtained under a 20x objective. Stack confocal images were then processed using the image processing package Fiji [89].

First, image type was converted to RGB, and then stack images of cell nuclei stained with Hoechst were collapsed to obtain a maximum 2D image projection, which were used to draw regions of interest (ROIs), delimiting each DG region (Figure 3.2.). SGZ was delimited as a region expanding 12.5 µm around the inner limit of the GCL.

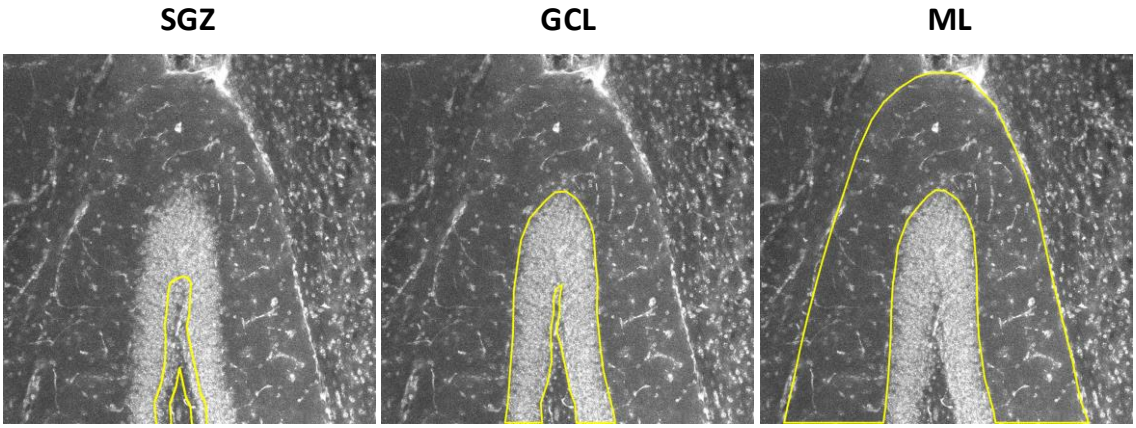

Figure 3.2.: Maximum projection representative images of nuclei stained with Hoechst 33342. In yellow is represented the outlined regions of interest (ROIs) of SGZ, GCL and ML of the DG.

In order to perform 3D reconstruction of blood vessels, the obtained ROIs were then applied on PECAM stack images and blood vessels were traced inside the limits of each corresponding ROI using the Simple Neurite Tracer plugin of Fiji (Figure 3.3.) [90].

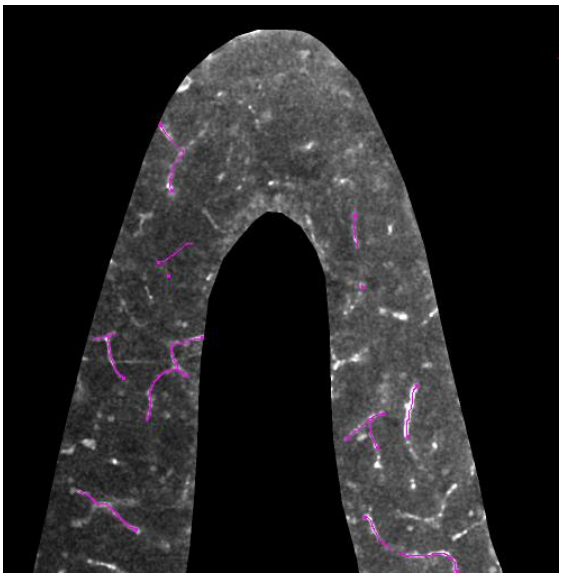

Figure 3.3.: Representative image of 3D reconstruction of blood vessels structure using Simple Neurite Tracer plugin from Fiji program. In pink are represented some traces of blood vessels that were drawn in the ML of the DG.

3.2.2. Blood vessels volume analysis in DG

To analyze blood vessels volume, the filling of the pixels located around the blood vessels traces previously obtained, was performed according to their intensity values (Figure 3.4.). The "3D object counter" plugin for Fiji [91] was used to perform an automatic analysis of blood vessels volume in each ROI, as well as the ROIs volume. The data obtained from this automatic analysis were then used to calculate the percentage of blood vessels volume in the SGZ, GCL and ML in relation to the volume of the corresponding region.

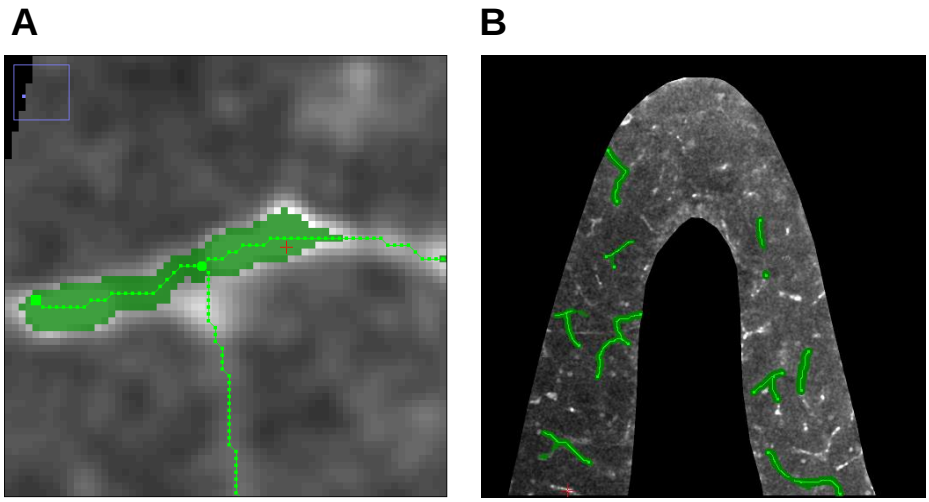

Figure 3.4.: Representative images of 3D reconstruction of blood vessels volume obtained by Fiji program processing. (A) In dark green, is represented the filling of pixels around the blood vessels traces (in light green), according to the pixel intensity values of PECAM staining. (B) Example of the final filling of the traces.

3.2.3. Blood vessels complexity analysis in DG

The structure and complexity of the reconstructed blood vessels was analyzed with "Analyze Skeleton" Fiji plugin [92], integrated into "Simple Neurite Tracer" plugin. This tool provided the number of branches and junctions (Figure 3.5.), as well as the length of blood vessels in each ROI. The linear density of blood vessels branches was calculated using the number of blood vessels branches in relation to the blood vessels length for each ROI and was expressed as blood vessel branches/µm. In the same way, the linear density of blood vessels junctions was determined in relation to blood vessels length in each ROI and the results expressed as blood vessel junctions/µm.

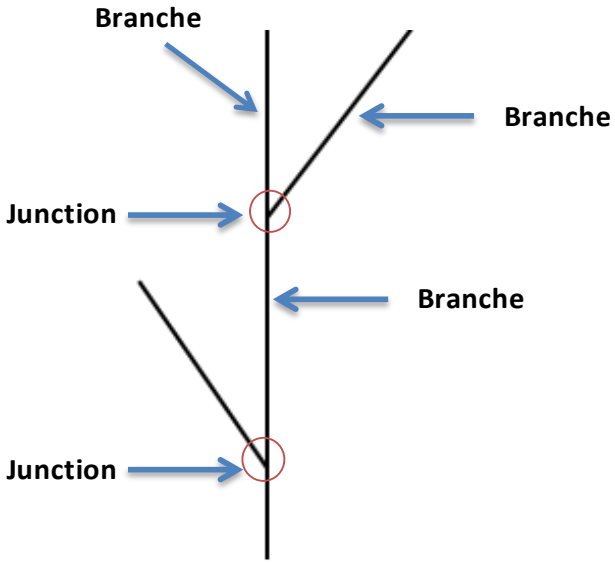

Figure 3.5.: Schematic representation of branches and junctions.

3.2.4. Blood vessels functionality analysis in DG

For the analysis of blood vessels functionality in DG, the same confocal images referred above were used. In addition, 8 confocal images from the cerebellum (4 images for each genotype) were also acquired as a control of the specificity of the data obtained in the hippocampus, since the cerebellum is unafected in AD [93].

The analysis of blood vessels functionality was carried out with Fiji program in each region of the DG. On the processed images of each DG region, obtained from the fill of pixels around traces, a threshold was set to the maximum to enable the automatic segmentation of all blood vessels. ROIs of the filled pixels on the processed images were created based on pixel intensity, by using the Analyze Particle command and, then applied to the corresponding dextran thresholded image. Then, the quantification of blood vessels functionality was calculated by the percentage of dextran (corresponding to functional vessels) colocalizing with PECAM, which identifies all the vessels in the tissue.

3.2.5. Analysis of blood vessels integrity by Evans blue leakage quantification in DG

In order to assess blood vessels integrity, confocal image stacks were obtained (23 for 3xTg-AD and 67 for NonTg) from hippocampal sections under a 40x oil immersion objective. The analysis of confocal images was carried out with Fiji program to quantify Evans blue staining intensity inside and outside the blood vessels in each region of the DG. 9 confocal image stacks were also obtained from hippocampal sections of NonTg treated mouse with mannitol (n=1) and from cerebellum (9 for 3xTg-AD and 9 for NonTg) that was used as a control. Stacks corresponding to the Evans blue fluorescent channel were collapsed to obtain a 2D image with maximal projection. Contours were manually traced around blood vzessels. ROI-circles (with a diameter of 4.61 µm) were placed around the blood vessels boundaries and the fluorescence intensity was measured for all ROIs. The ratio of Evans blue dye intensity outside/inside blood vessels was calculated as a measure of Evans blue leakage. A significant increase in this ratio was considered as blood vessels loss of integrity.

3.2.6. Analysis of neural stem cells colocalization with vessels

The analysis of the colocalization of neural stem cells with vessels was performed using confocal image stacks (21 for 3xTg-AD and 14 for NonTg), from hippocampal sections under a 40x oil immersion objective. Stem cells were identified as positive cells for Sox2 and Nestin, with a radial morphology [94]. For the segmentation of these cells, maximum projection of stack images was obtained and ROI manually drawn. Then, images were treated with "remove outliers" and "substract background" filters. A manual threshold was applied before the "analyze particle" [89] filter to finally obtain segmented binary images stacks, later used in the colocalization (Figure 3.5). For the segmentation of vessels, the original images were processed with "Gausssian Blur 3D" filter, followed by the "Find Peaks" plugin. Blood vessels in the images were further segmented with the filter "Analyze particles" and "3D object counter" plugin [91].

The quantification of colocalization between stem cells and vessels was calculated as the percentage of the Nestin area labelled for PECAM.

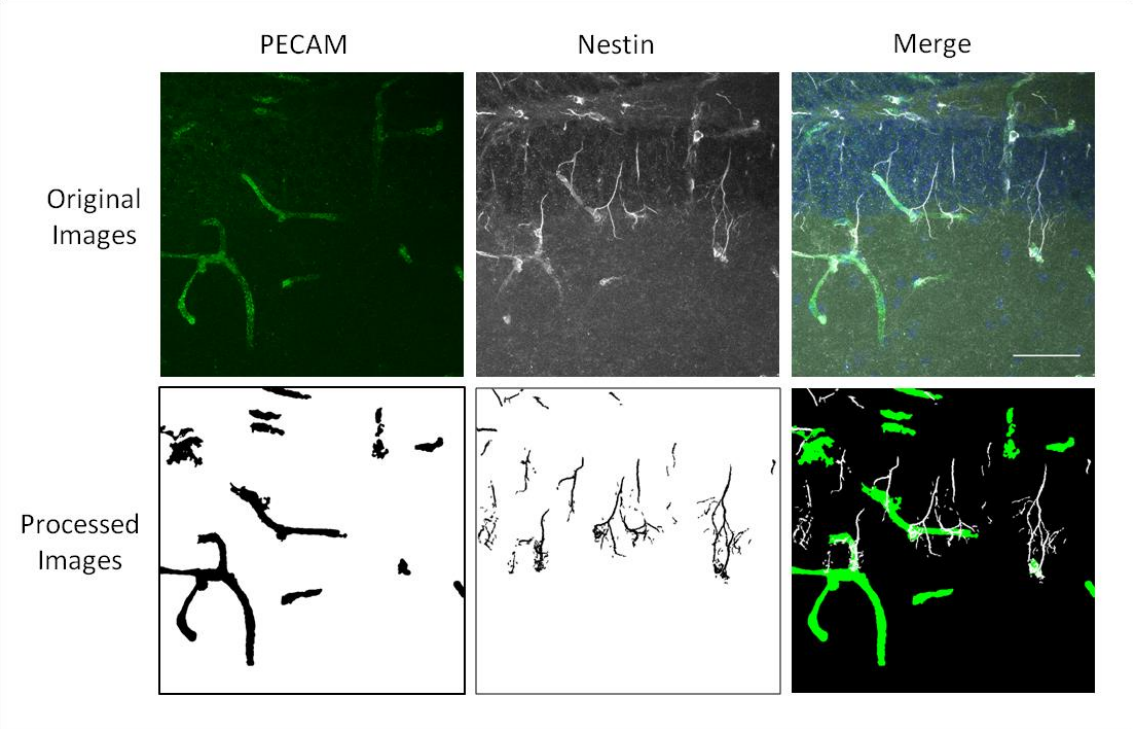

Figure 3.6: Representative confocal fluorescent images of blood vessels stained with platelet-endothelial cell adhesion molecule (PECAM; in green) antibody and stem cells stained with Nestin antibody (in white) (upper pannels) and the respective processed images (bottom panels) in hippocampal dentate gyrus. Cell nuclei are stained with Hoechst 33342 (in blue). Scale bar: 50 µm.

3.4. Statistical analysis

All data presented correspond to mean ± standard error of the mean (SEM) for all experiments. The statistical analysis was carried out with GraphPad Prism 5.0 (GraphPad software, San Diego, California, USA). Student's unpaired t test or two-way analysis of variance (2-way ANOVA) followed by Bonferroni *post-hoc* test for multiple comparisons were used to determine statistical significance (* $p < 0.05$, ** $p < 0.01$ and *** $p < 0.001$).

Chapter 4

Results

4.1. Microvasculature is affected in the DG of 3 month-old 3xTg-AD mice

To evaluate whether microvasculature is affected in 3 month-old 3xTg-AD mice, we first analyzed blood vessel volume and complexity, which was obtained through the quantification of the number of vessels branches and junctions. Functionality of blood vessels was then evaluated by using dextran Texas-red, an hydrophilic polysaccharide dye that labels functional vessels. Finally, we studied blood vessel integrity by determining blood vessel leakage of Evans blue dye.

4.1.1. Blood vessels volume is decreased in the SGZ of 3 month-old 3xTg-AD mice

In order to analyze the blood vessels volume in the DG of 3xTg-AD and NonTg mice, 3D reconstructions of blood vessels were obtained from confocal images of platelet-endothelial cell adhesion molecule (PECAM) staining. Figure 4.1A shows representative confocal fluorescent images of blood vessels stained with PECAM antibody (left panel) and the respective processed images (right panel). Analyzing the Figure 4.1B, it is possible to observe that there is a significant decrease of blood vessels volume in the SGZ of 3xTg-AD, when compared to NonTg mice. In turn, in the GCL and ML, it is also possible to observe a tendency to a decrease of the percentage of blood vessels volume on 3xTg-AD mice, which did not reach significance. No significant differences between 3xTg-AD and NonTg mice were obtained when considering the entire DG (Figure 4.1.C).

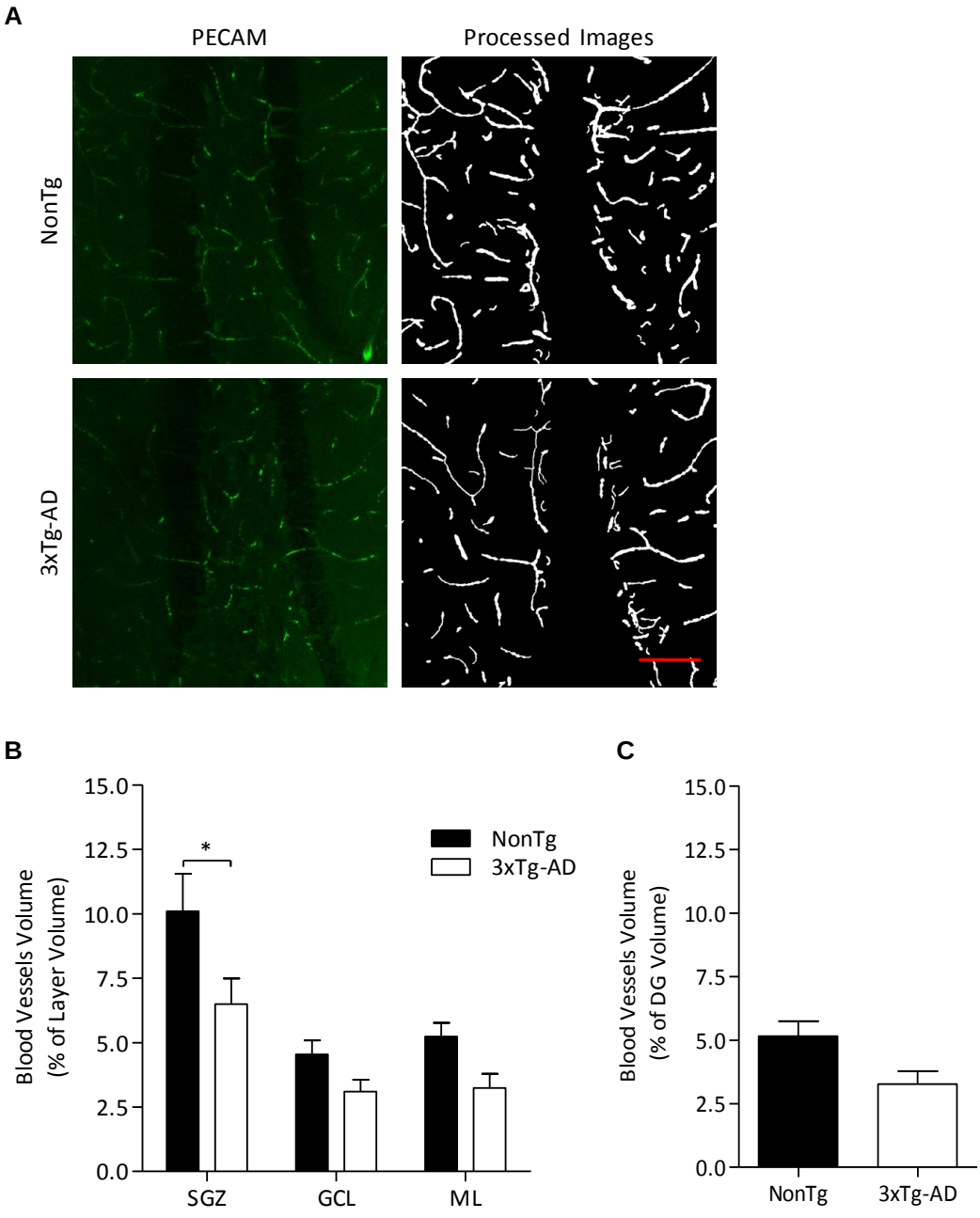

Figure 4.1: Blood vessels volume is decreased in the SGZ of 3 month-old 3xTg-AD mice. (A) Representative confocal fluorescent images of blood vessels stained with platelet-endothelial cell adhesion molecule (PECAM) antibody (left panels) and the respective processed images (right panels) in hippocampal dentate gyrus (DG) of 3 month-old 3xTg-AD and NonTg mice. Images were processed as described in chapter 2. Graphs represent blood vessel volume quantified and expressed as the percentage of the volume of each DG region (SGZ - subgranular zone; GCL – granule cell layer and ML – molecular layer) (B) and whole DG (C). The data are expressed as mean ± SEM (n=4). In (B) statistical significance was determined using two-way analysis of variance (2-way ANOVA) with Bonferroni's multiple comparison *post-hoc* test and in (C) statistical significance was analyzed using Student's unpaired t test. * $p < 0.05$. Scale bar: 100 µm.

4.1.2. Complexity of blood vessels is decreased in the DG of 3 month-old 3xTg-AD mice

For the analysis of blood vessel complexity the number of branches and junctions of blood vessels were quantified in the SGZ, GCL and ML of NonTg and 3xTg-AD mice. Blood vessels branches and junctions were quantified in relation to the blood vessels length (in µm) in each region. In Figure 4.2A, are depicted the confocal fluorescent images of blood vessels stained with PECAM antibody (left panel) and the respective processed images (skeleton) showing blood vessels branches, in a magnified region of the SGZ and ML. Results show a significant decrease in the number of branches per µm of blood vessels in SGZ and ML of 3xTg-AD compared to the respective controls, being more pronounced in the SGZ. In the GCL no significant decrease was observed. Furthermore, when analyzing the entire DG a significant decrease in this parameter was observed in 3xTg-AD mice (Figure 4.2C).

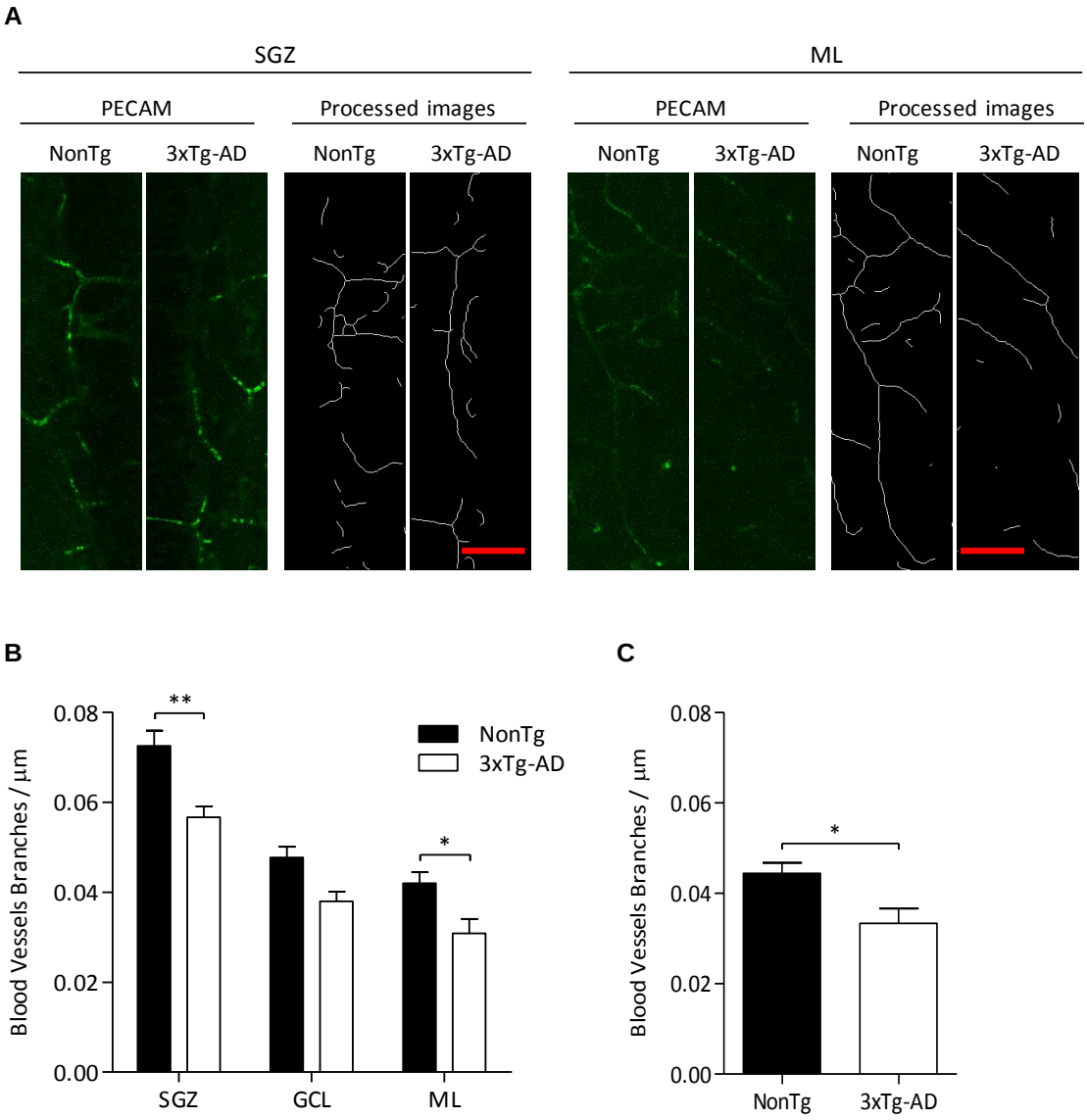

Figure 4.2: Blood vessels branches are decreased in the SGZ and ML of 3xTg-AD mice. (A) Magnification of a selected area of SGZ and ML regions of the DG from the images represented in the figure 4.1A. Blood vessels branches were quantified in relation to the blood vessels length (blood vessel branches/µm) in the three DG regions (SGZ - subgranular zone; GCL – granule cell layer and ML – molecular layer) (B) and the whole DG (C) of 3 month-old 3xTg-AD and NonTg mice. The data are expressed as mean ± SEM (n=4). In (A) statistical significance was determined using two-way analysis of variance (2-way ANOVA) with Bonferroni's multiple comparison *post-hoc* test and in (B) statistical significance was analyzed using Student's unpaired t test. * $p < 0.05$; ** $p < 0.01$. Scale bar: 100 µm.

In addition, a decrease in the number of junctions per µm of blood vessels can be observed in the SGZ of 3xTg-AD, when compared to NonTg mice (Figure 4.3A). No significant differences are found in the GCL, ML or when considering the entire DG, between the two genotypes.

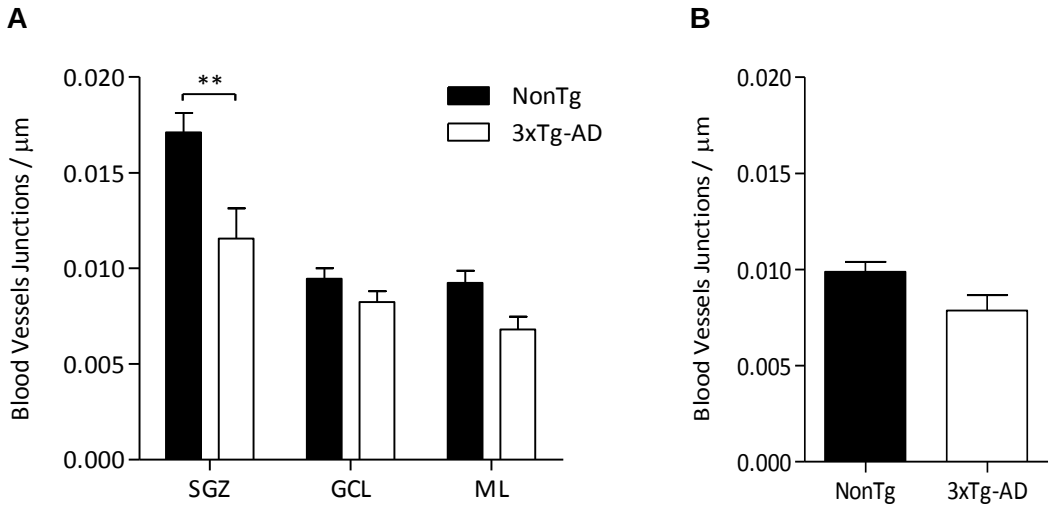

Figure 4.3: Blood vessels junctions are decreased in the SGZ of 3xTg-AD mice. Blood vessels junctions were quantified in relation to the blood vessels length (blood vessel branches/µm) in the three DG regions (SGZ - subgranular zone; GCL – granule cell layer and ML – molecular layer) (A) and the whole DG (B) of 3 month-old 3xTg-AD and NonTg mice. The data are expressed as mean ± SEM (n=4). In (A) statistical significance was determined using two-way analysis of variance (2-way ANOVA) with Bonferroni's multiple comparison *post-hoc* test and in (B) statistical significance was analyzed using Student's unpaired t test. * $p < 0.05$; ** $p < 0.01$.

4.1.3. Loss of blood vessels functionality in the DG of 3 month-old 3xTg-AD mice

To assess blood vessels functionality in the SGZ, GCL and ML of the DG of 3xTg-AD and control mice colocalization between dextran-positive vessels (functional vessels) and PECAM-positive vessels (functional + non-functional vessels) was determined (Figure 4.4). A significant decrease of the percentage of dextran/PECAM colocalization was found in all the three regions of the DG of 3xTg-AD mice compared to NonTg mice (Figure 4.4A and B). This decrease in SGZ, GCL and ML results in a decrease in the entire DG (Figure 4.4A and C). Furthermore, we were interested in elucidating whether these observations were specific to the DG. To achieve this, we analyze the colocalization between functional vessels and all the vessels in the cerebellum, an area that is not affected in AD [93] (Figure 4.4A and C). A significant increase in the percentage of dextran/PECAM colocalization was observed in the cerebellum of 3xTg-AD mice, when compared to the cerebellum of NonTg mice, indicating that loss of vessels functionality is specific of the DG of 3xTg-AD mice.

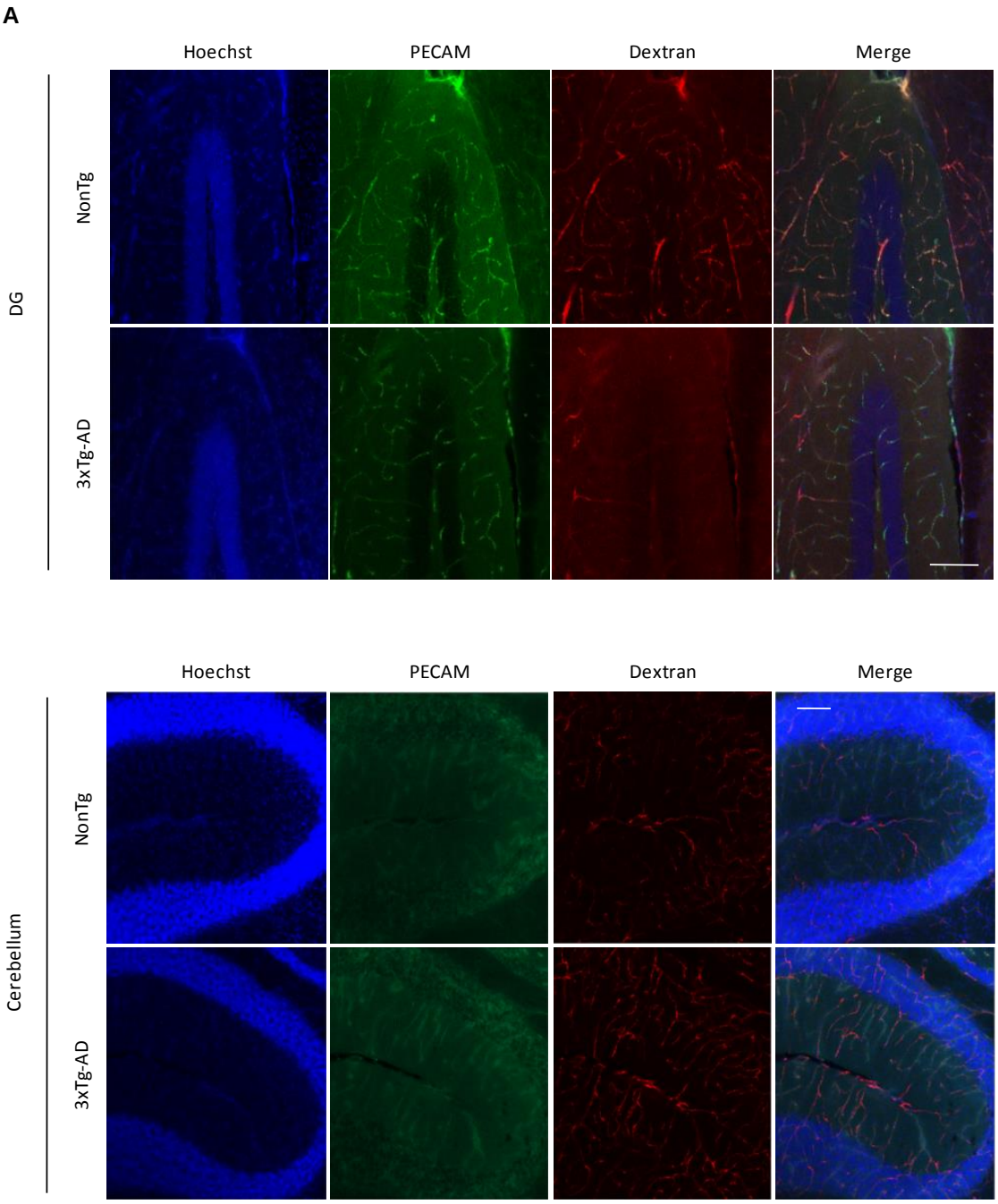
A
Hoechst
PECAM
Dextran
Merge
DG
NonTg
3xTg-AD
Hoechst
PECAM
Dextran
Merge
Cerebellum
NonTg
3xTg-AD

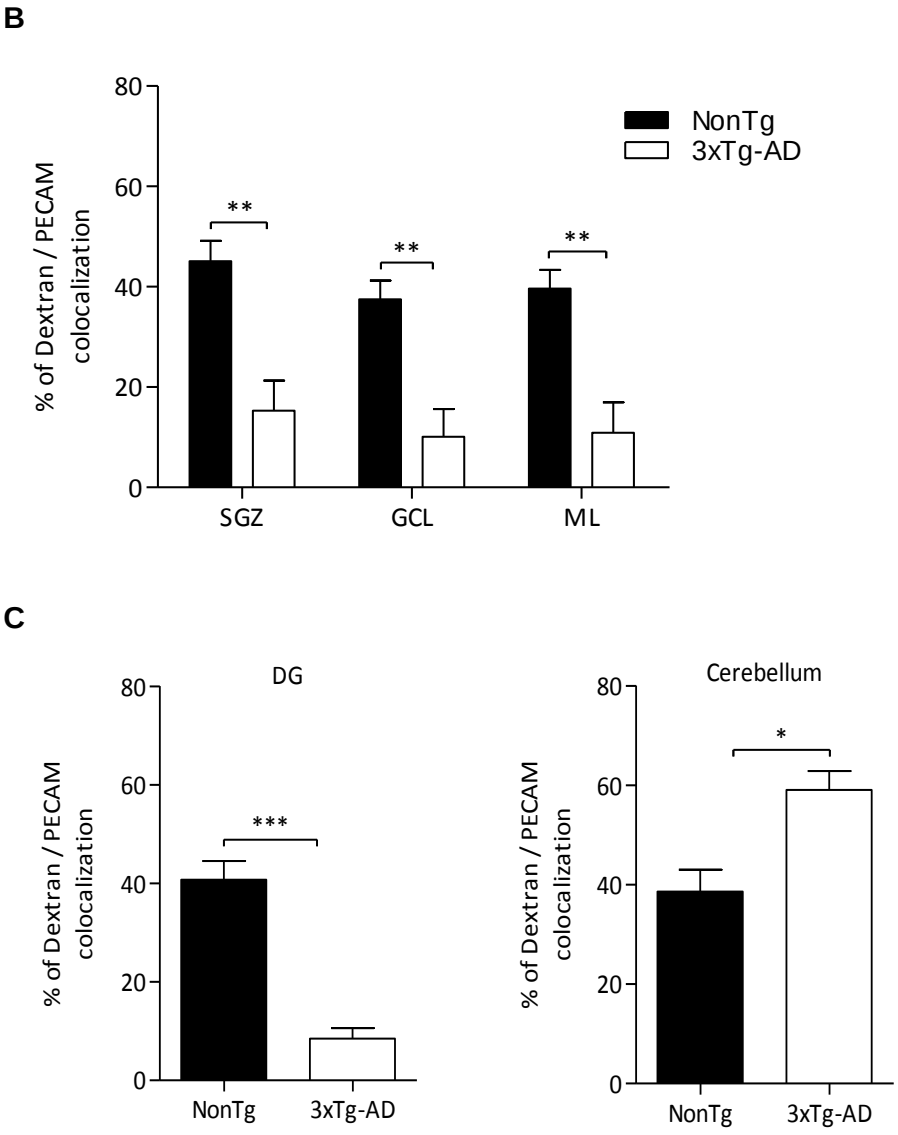

Figure 4.4: Functionality of blood vessels is decreased in the DG of 3 month-old 3xTg-AD mice. (A) Representative confocal images of hippocampal DG and cerebellum blood vessels stained with PECAM (in green) and dextran (in red) in NonTg and 3xTg-AD mice. Nuclei were stained with Hoechst33342 (in blue). Blood vessel functionality was analyzed through the quantification of the percentage of dextran colocalization with PECAM in the three different regions of the DG (SGZ - subgranular zone; GCL – granule cell layer and ML – molecular layer) (B), of the whole DG and cerebellum (C) of 3 month-old 3xTg-AD and NonTg mice. The data are expressed as mean ± SEM (n=4). In (B) statistical significance was determined using two-way analysis of variance (2-way ANOVA) with Bonferroni's multiple comparison *post-hoc* test and in (C) statistical significance was analyzed using Student's unpaired t test. * $p < 0.05$; ** $p < 0.01$; *** $p < 0.001$. Scale bar: 100 µm.

4.1.4. Blood vessels integrity is affected in the DG of 3 month-old 3xTg-AD mice

In order to assess to the integrity of blood vessels in the SGZ, GCL and ML of the DG, Evans blue, a dye that binds to serum albumin (a protein that in normal physiological conditions do not cross the BBB) was used. As a consequence, Evans blue remains inside intact vessels, while in damaged vessels Evans blue leaks out of vessels. Vessel integrity can thus be evaluated by determining the ratio of Evans blue dye intensity outside and inside blood vessels (Figure 4.5). To optimize our protocol, we first evaluate whether we could measure Evans blue leakage in a situation of BBB disruption. With this purpose, NonTg mice were treated with mannitol, a sugar alcohol that induces the osmotic opening of the BBB [88]. This compound induced a significant increase in Evans blue leakage of blood vessels in the three areas of the DG of NonTg-mice (Figure 4.5A and B). When analyzing blood vessel integrity in 3xTg-AD mice, a significant increase of Evans blue dye leakage was observed in SGZ and ML, when compared to the NonTg mice (Figure 4.5A and C), which contributed to the increase found in the entire DG (Figure 4.5D). No significant alteration in vessel integrity was observed in the GCL of 3xTg-AD mice (Figure 4.5A and C). We also compared these data with the ones obtained in the cerebellum and verified that no alteration occurs in the vessels of this brain area (Figure 4.5D), indicating that the loss of integrity of blood vessels is specific of the DG of 3xTg-AD mice.

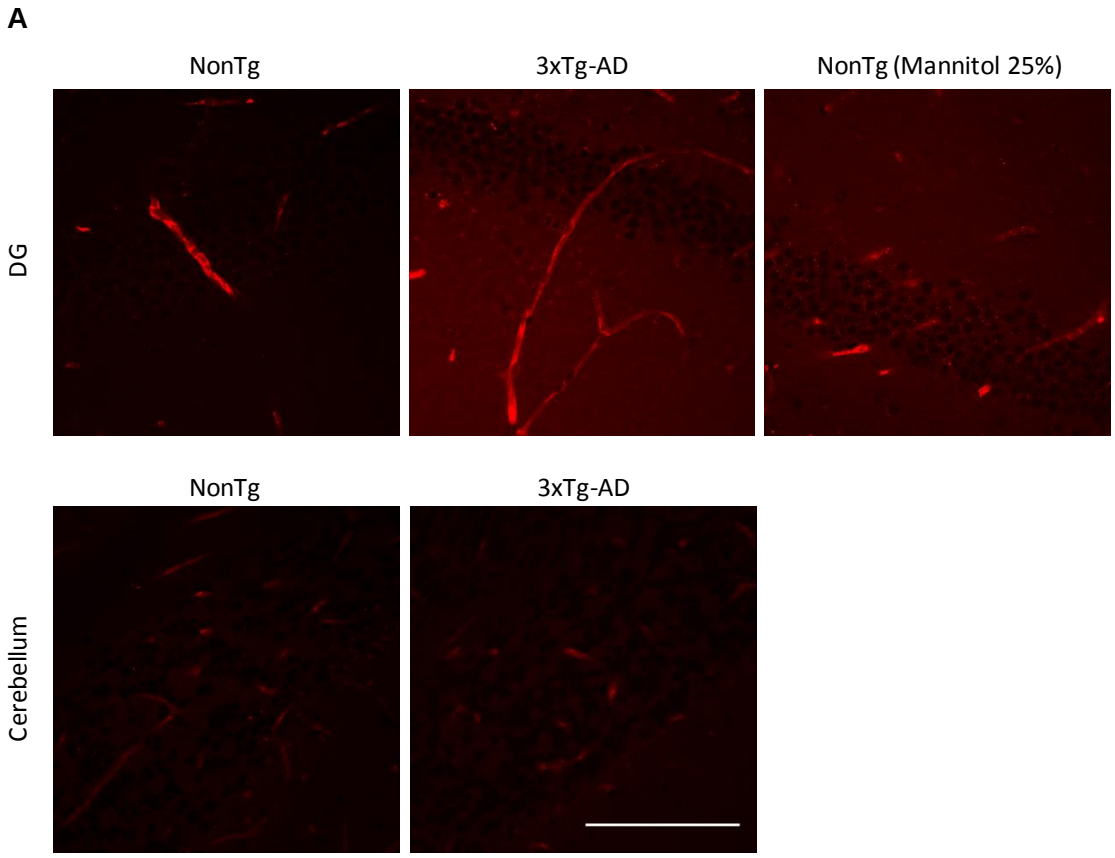
A
NonTg
3xTg-AD
NonTg (Mannitol 25%)
DG
NonTg
3xTg-AD
Cerebellum

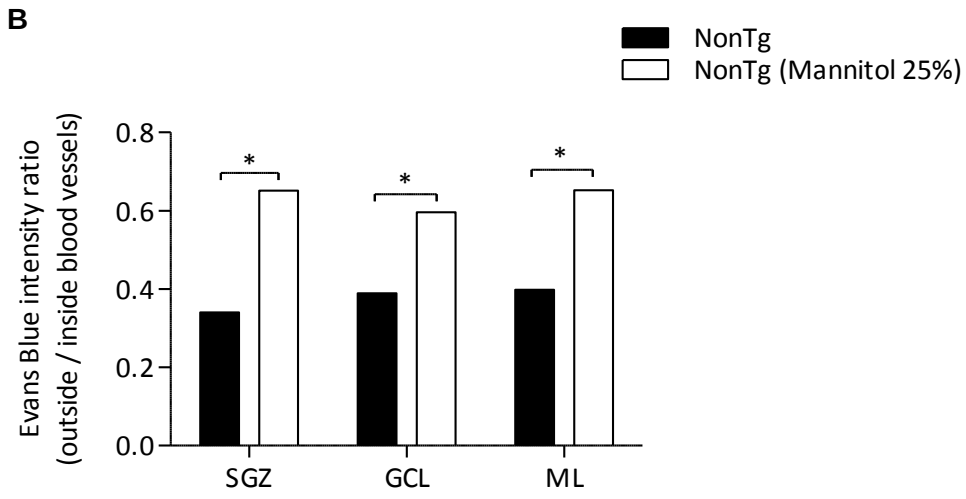
B
NonTg
NonTg (Mannitol 25%)
Evans Blue intensity ratio
(outside / inside blood vessels)
0.8
0.6
0.4
0.2
0.0
*
*
*
SGZ
GCL
ML

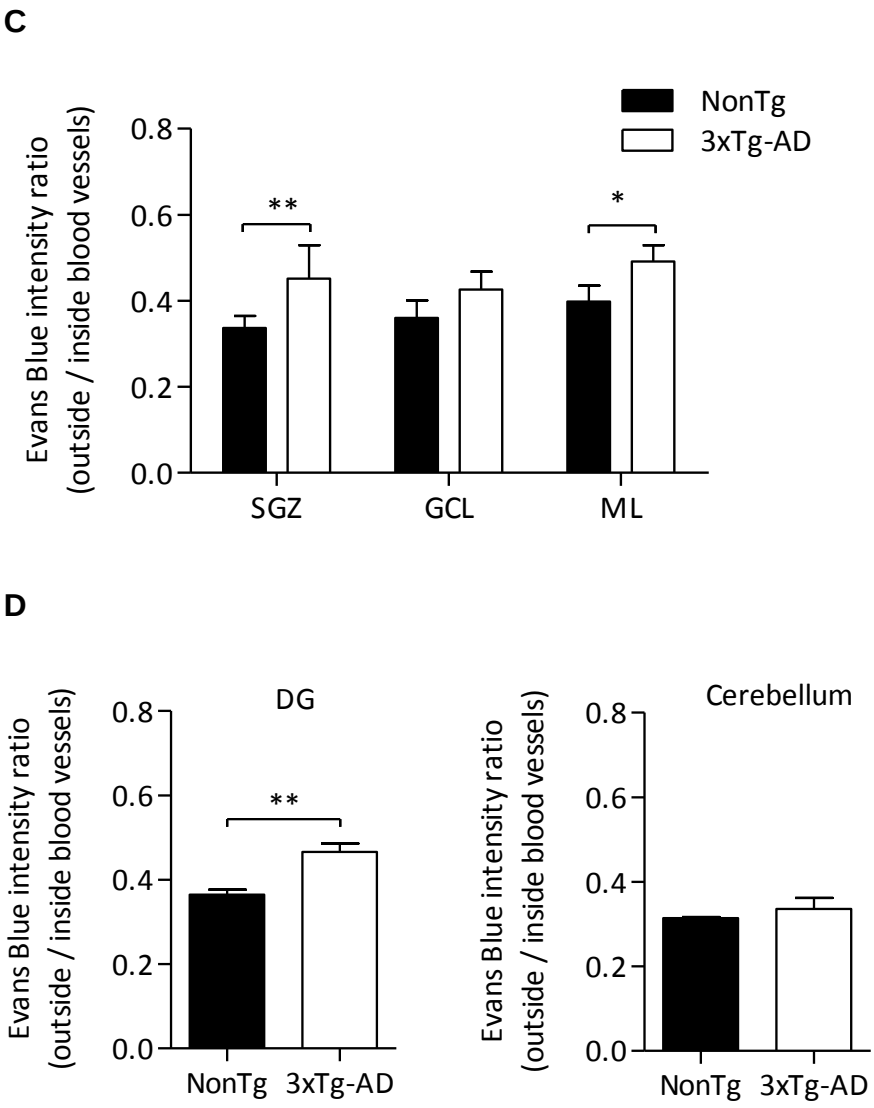

Figure 4.5: Blood Vessels leakage is increased in the SGZ and ML of 3 month-old 3xTg-AD mice. Blood vessel integrity was determined by calculating the ratio between Evans blue intensity outside and inside the vessels in the hippocampal dentate gyrus (DG) and cerebellum of 3 month-old 3xTg-AD and NonTg mice. (A) Representative confocal images of Evans blue staining in the DG of 3xTg-AD and untreated or 25% mannitol-treated NonTg mice. (B) Evans blue leakage was analyzed in the three different regions of the DG (SGZ - subgranular zone; GCL – granule cell layer and ML – molecular layer). (C) As a positive control, a NonTg mouse was treated with 25 % mannitol and Evans blue intensity analyzed in the different regions of the DG. (D) Evans blue leakage was analyzed in the whole DG and in the cerebellum of 3xTg-AD and NonTg mice. The data are expressed as mean ± SEM (n=6 for NonTg; n=3 for 3xTg-AD). In (B) and (C) statistical significance was determined using two-way analysis of variance (2-way ANOVA) with Bonferroni's multiple comparison *post-hoc* test and in (D) statistical significance was analyzed using Student's unpaired t test. * $p < 0.05$; ** $p < 0.01$. Scale bar: 100 µm.

4.1.5. Neural stem cells proximity to blood vessels is increased in 3 month-old 3xTg-AD mice

In the adult SGZ neurogenic niche, vessels play a fundamental role due to its proximity to neural stem cells and since neural progenitor cells proliferate together with endothelial precursors [32]. As an attempt to explore the relationship between neurogenesis and the microvasculature in 3xTg-AD mice, we analyze the proximity of stem cells to blood vessels by quantifying the colocalization of radial nestin-positive cells (stem cells) and blood vessels stained with PECAM (Figure 4.6). Stem cells are radial cells that have their cell body within the SGZ and send projections that cross the GCL, reaching the ML. No alterations were observed in the % of nestin area stained with PECAM in the SGZ and GCL of 3xTg-AD mice, when compared to NonTg mice (Figure 4.6A and B). Interestingly, a significant increase of the colocalization of stem cells with blood vessels was found in the ML of 3xTg-AD mice (Figure 4.6A red arrows and B). This increase in the proximity of stem cells to blood vessels was not reflected on the entire DG (Figure 4.6C).

These data further suggest that the vasculature interacts with stem cells and may play a role in the impairment of neurogenesis that occurs in 3 month-old 3xTg-AD mice (unpublished data from our laboratory).

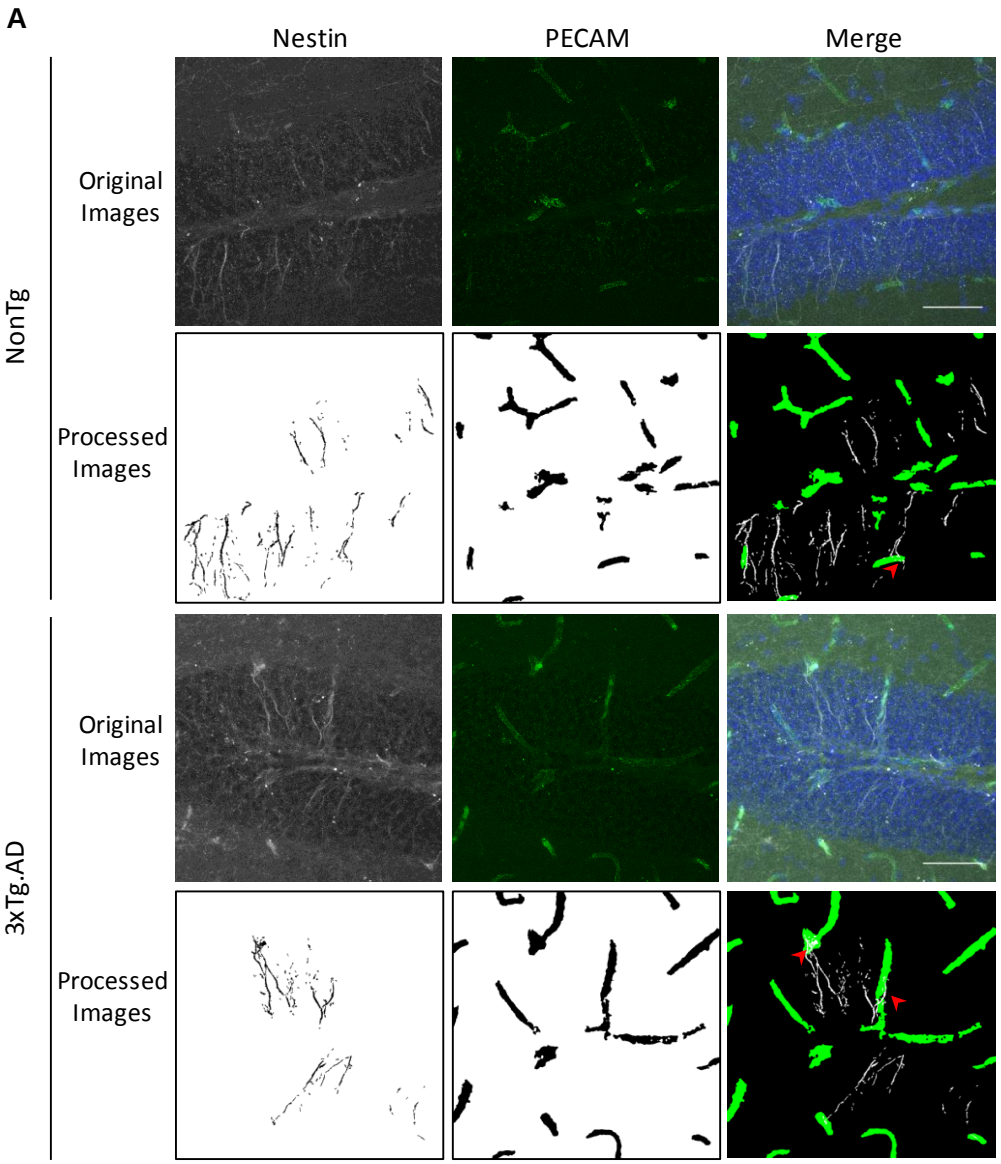
A
Nestin
PECAM
Merge
NonTg
Original Images
Processed Images
3xTg.AD
Original Images
Processed Images

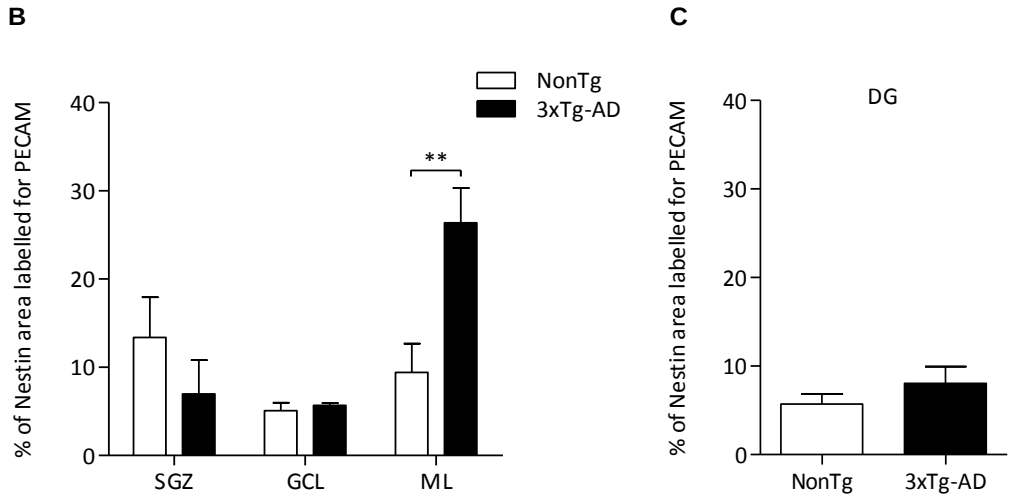

Figure 4.6: The proximity of stem cells to blood vessels is increased in the ML of 3xTg-AD mice. (A) Representative confocal fluorescent images of blood vessels stained with platelet-endothelial cell adhesion molecule (PECAM; in green) antibody and stem cells stained with Nestin antibody (in white) and the respective processed images in DG. Stem cells were identified as positive cells for Sox2 (not represented in the figure) and Nestin, with a radial morphology. Cell nuclei are stained with Hoechst 33342 (in blue). Red arrows indicate stem cells and vessels colocalization. Proximity of stem cells to blood vessels was analyzed as described in chapter 2, by quantification of the colocalization between stem cells (nestin-positive cells) and blood vessels (PECAM-positive cells) in the three different regions of the DG (SGZ - subgranular zone; GCL – granule cell layer and ML – molecular layer) (B) and the whole DG (C) of 3 month-old 3xTg-AD and NonTg mice. The data are expressed as mean ± SEM (n=3). In (B) statistical significance was determined using two-way analysis of variance (2-way ANOVA) with Bonferroni's multiple comparison *post-hoc* test. ** $p < 0.01$. Scale bar: 50 µm.

Chapter 5

Discussion

Evidences point to a vascular involvement in the origin of AD pathology. Indeed, cerebrovascular changes are thought to arise before the onset of this neuropathological disorder [36, 51]. A recent study conducted by Minh Do, et al. (2014), performing an *in situ* perfusion of [^{14}C]-sucrose (a marker of cerebrovascular space), showed a reduction in cerebral vascular volume in the hippocampus 6 month-old 3xTg-AD mice , before the appearance of Aβ plaques and tangles, which persists in aged animals [95]. This study complies with the decrease in the volume of blood vessels that we observed in the SGZ of the DG of 3xTg-AD mice. For a better characterization of cerebrovascular structural changes in the DG, we also assessed the blood vessels complexity in this specific region and observed an evident reduction in the number of branches and junctions per length of blood vessels in the DG of this AD mouse model. Thus, we can suggest that in the hippocampal DG the volume of microvasculature appear to be affected in AD.

Several studies have shown the deposition of Aβ peptide in the cerebrovasculature of AD transgenic mice and AD patients [96-97], which can have a detrimental effect on ECs viability, affecting blood vessels function. This Aβ can be produced by ECs themselves or by the brain parenchyma, or be transported by circulating blood [98-99]. Aβ may exert multiple effects on ECs, namely affecting Ca^{2+} and redox homeostasis, endoplasmic reticulum function and proteostasis, leading to ECs dysfunction [100-102]. Moreover in response to Aβ peptide accumulation, neuroinflammatory vascular responses are triggered through the activation of brain endothelium, pericytes, astrocytes and perivascular microglia recruitment [52, 103-104]. Subsequently, activated cells secrete pro-inflammatory cytokines and vasoactive substances, reducing CBF, which could contribute to cognitive defects (Deane, 2003). For example, astrocytes end feet appear to be intimately close to the vascular surface and are involved in the regulation of vascular strength and in the CBF [49]. Thus, inflammation triggered by Aβ can lead to astrocytic end feet swelling causing vascular constriction [105-106].

To our knowledge the accumulation of Aβ in vessels in the 3xTg-AD mice has not been described. But considering that 3xTg-AD mice present an intraneuronal accumulation of soluble Aβ peptides at 3 months of age, thought to be involved in early synaptic dysfunction [27], it is possible that Aβ may be involved in the cerebrovascular

alterations that were founded. Further experiments will be performed in the future to elucidate whether Aβ is produced by or accumulate in blood vessels of these transgenic mice, contributing to the observed alterations. The AD-related structural cerebrovascular changes, namely the reduction of branches and junctions in blood vessels that we showed to occur in the DG of 3xTg-AD mice can somehow explain the altered function of blood vessels. Deficient vascular innervations due to loss of blood vessels complexity and volume can compromise the perfusion rate and blood supply to specific regions in the brain, contributing to an altered regional brain function, including neuronal damage [49]. As a consequence, inflammation can be triggered in response to neuronal degeneration and also contribute to BBB disruption. These structural cerebrovascular changes can thus affect blood supply to the brain and cause regional EC damage [49]. We can also suggest that the accumulation of Aβ peptide in the outer side of the basement membrane of blood vessels wall can affect the functionality loss observed in the DG.

Another relevant contribution for the study of cerebrovascular changes in AD is the assessment of the integrity of blood vessels in the DG. Our results indicate a substantial increase in the leakage of blood vessels in the DG, suggesting that blood vessels integrity is compromised. Several events may be in the origin of breakdown of cerebral microvessels in AD: alterations in the neurovascular unit, including decreased mitochondrial density in ECs, accumulation of extracellular matrix components in the vascular basement membrane, loosening of tight junctions, changes in astrocytic end feet and thickening of the vessel wall, accompanied by a loss of elasticity affecting brain perfusion [49, 52, 107]. Causes arising from the loss of blood vessel integrity may include synaptic and neuronal dysfunction due to the compromised CNS homeostasis [104, 107].

In the adult SGZ neurogenic niche, blood vessels play an essential role in the regulation of neurogenesis by providing circulating and secreted factors [32]. In fact, neural stem/progenitor cells appear to be in a close association with blood vessels, which allow constant access to circulating signaling molecules and nutrients [32, 68]. Moreover, in the SGZ, neurogenesis occurs accompanied by a vascular recruitment indicating an interdependent relationship between neurogenesis and the vasculature

[68]. The generation of new neurons in the hippocampus has been thought to play a role in memory and learning functions [63, 77, 108]. Growing evidences indicate that a decline in the neurogenesis may underlie cognitive impairments associated with aging and AD [76, 85]. Experiments performed by Rodríguez and co-workers (2008) showed a reduction in the proliferation of cells in the GCL of the DG in 3xTg-AD mouse model, from 6 until at least 12 months of age [83]. Recent findings from our group demonstrated a decrease in the number of stem cells, an increased number of astrocyte progenitors and a marked decrease in neuroblasts in the DG of 3 month-old 3xTg-AD mice. These observations are consistent with impairment of hippocampal neurogenesis as suggested by studies using other transgenic models [109-111]. Due to the high relationship between blood vessels and NSCs in the vascular niche it is possible that impairment in neurogenesis is related to dysfunctional vasculature. In fact, the decrease in the volume and complexity of blood vessels that we observed to occur in the SGZ and ML, may lead to a reduction in the supply of factors to both NSCs and progenitor cells, compromising both proliferation and differentiation. The increased proximity between NSCs and blood vessels in the ML observed in 3xTg-AD mice can be thus seen as a response mechanism in the search for survival of the remaining NSCs in the DG neurogenic niche. Recently, an interesting study showed that factors found in young blood can remodulate the vasculature, promoting neurogenesis in aged mice [112]. This study further supports that strategies directed to the improvement of the normal vasculature function may promote neurogenesis in the DG and rescue cognitive deficits in AD. A profound understanding of the dynamic between blood vessels and NSCs/progenitors, and its role in AD is presently absent. Therefore, this field of research constitutes a strong challenge due to its high impact and novelty. We strongly believe that the data here presented raise several questions to be explored. To further complement the study here presented, many different future works can be proposed: i) measure the distance of stem/progenitor cells and neuroblasts to blood vessels; ii) investigate the presence of Aβ in vessels in the DG; iii) quantify VEGF levels, since it is a regulation of angiogenesis and neurogenesis in the neurogenic niche; iv) characterize microvasculature and neurogenesis in younger animals; v) replicate this study in another transgenic mouse model of AD.

The data presented in this thesis support vascular alterations as an early event in the progression of AD and the existence of interplay between blood vessels and NSCs, possibly contributing for the impairment of neurogenesis that occurs in this neurodegenerative disease.

These findings may bring in the future new therapeutic perspectives for the treatment of AD.

Chapter 6

Conclusion

Considering our work hypothesis, the main objectives and the results obtained in 3 month-old 3xTg-AD mice models of AD, it is possible to conclude that:

- Blood vessels volume is decreased in the SGZ of the DG;
- Complexity of the vasculature is reduced in the SGZ and ML of the DG;
- Functionality of blood vessels is lost in the SGZ, GCL and ML of the DG;
- Integrity of blood vessels is reduced in the SGZ and ML of the DG;
- NSCs processes lay closer to vessels in the ML of the DG.

Summarizing, we conclude that microvasculature alterations in the hippocampal DG are an early event and that blood vessels and NSCs closely interact, which may contribute to neurogenesis impairment that occurs in AD.

Chapter 7

References

1. Cummings, J.L., *Alzheimer's disease.* N Engl J Med, 2004. **351**(1): p. 56-67.
2. Brookmeyer, R., et al., *Forecasting the global burden of Alzheimer's disease.* Alzheimers Dement, 2007. **3**(3): p. 186-91.
3. Mayeux, R., *Epidemiology of neurodegeneration.* Annu Rev Neurosci, 2003. **26**: p. 81-104.
4. An, Y.H., et al., *Main hypotheses, concepts and theories in the study of Alzheimer's disease.* Life Science Journal-Acta Zhengzhou University Overseas Edition, 2008. **5**(4): p. 1-5.
5. Forstl, H. and A. Kurz, *Clinical features of Alzheimer's disease.* Eur Arch Psychiatry Clin Neurosci, 1999. **249**(6): p. 288-90.
6. Gogia, P.P. and N. Rastogi, *Clinical Alzheimer Rehabilitation*. 2009, New York: Springer Publishing Company.
7. Ahmad, S.I., *Diseases of DNA Repair: Advances in Experimental Medicine and Biology*. Vol. 685. 2010, New York: Springer. 34-44.
8. Martínez-Murcia, F.J., et al., *Computer Aided Diagnosis tool for Alzheimer's Disease based on Mann–Whitney–Wilcoxon U-Test.* Expert Systems with Applications, 2012. **39**(10): p. 9676-9685.
9. Humpel, C., *Identifying and validating biomarkers for Alzheimer's disease.* Trends Biotechnol, 2011. **29**(1): p. 26-32.
10. Mucke, L., *Neuroscience: Alzheimer's disease.* Nature, 2009. **461**(7266): p. 895-7.
11. Singh, M., et al., *Acetylcholinesterase inhibitors as Alzheimer therapy: from nerve toxins to neuroprotection.* Eur J Med Chem, 2013. **70**: p. 165-88.
12. Dominguez, E., et al., *Management of moderate to severe Alzheimer's disease: focus on memantine.* Taiwan J Obstet Gynecol, 2011. **50**(4): p. 415-23.
13. Johnson, K.A., et al., *Brain imaging in Alzheimer disease.* Cold Spring Harb Perspect Med, 2012. **2**(4): p. a006213.
14. Blennow, K., M.J. de Leon, and H. Zetterberg, *Alzheimer's disease.* Lancet, 2006. **368**(9533): p. 387-403.
15. Swerdlow, R.H., *Pathogenesis of Alzheimer's disease.* Clin Interv Aging, 2007. **2**(3): p. 347-59.
16. Ballard, C., et al., *Alzheimer's disease.* Lancet, 2011. **377**(9770): p. 1019-31.
17. Silva, T., et al., *Alzheimer's disease, enzyme targets and drug discovery struggles: from natural products to drug prototypes.* Ageing Res Rev, 2014. **15**: p. 116-45.
18. Baum, L.W., *Sex, hormones, and Alzheimer's disease.* J Gerontol A Biol Sci Med Sci, 2005. **60**(6): p. 736-43.
19. Tayeb, H.O., et al., *Pharmacotherapies for Alzheimer's disease: beyond cholinesterase inhibitors.* Pharmacol Ther, 2012. **134**(1): p. 8-25.
20. Dawbarn, D. and S.J. Allen, *Molecular genetics of Alzheimer's disease*, in

Neurobiology of Alzheimer's Disease, O.U. Press, Editor. 2007: Oxford. p. 59-79.
21. Swerdlow, R.H., J.M. Burns, and S.M. Khan, *The Alzheimer's disease mitochondrial cascade hypothesis: Progress and perspectives.* Biochim Biophys Acta, 2014. **1842**(8): p. 1219-1231.
22. Pereira, C., et al., *Cell degeneration induced by amyloid-beta peptides: implications for Alzheimer's disease.* J Mol Neurosci, 2004. **23**(1-2): p. 97-104.
23. Maccioni, R.B., et al., *The revitalized tau hypothesis on Alzheimer's disease.* Arch Med Res, 2010. **41**(3): p. 226-31.
24. Mohandas, E., V. Rajmohan, and B. Raghunath, *Neurobiology of Alzheimer's disease.* Indian J Psychiatry, 2009. **51**(1): p. 55-61.
25. de la Torre, J.C., *Vascular risk factor detection and control may prevent Alzheimer's disease.* Ageing Res Rev, 2010. **9**(3): p. 218-25.
26. Spires, T.L. and B.T. Hyman, *Transgenic models of Alzheimer's disease: learning from animals.* NeuroRx, 2005. **2**(3): p. 423-37.
27. Oddo, S., et al., *Triple-transgenic model of Alzheimer's disease with plaques and tangles: intracellular Abeta and synaptic dysfunction.* Neuron, 2003. **39**(3): p. 409-21.
28. Oddo, S., et al., *Amyloid deposition precedes tangle formation in a triple transgenic model of Alzheimer's disease.* Neurobiol Aging, 2003. **24**(8): p. 1063-70.
29. Mota, *NMDA-receptors-associated events and oxidative stress in models of Alzheimer´s disease*. 2013, University of Coimbra, Portugal.
30. Kalaria, R.N., R. Akinyemi, and M. Ihara, *Does vascular pathology contribute to Alzheimer changes?* J Neurol Sci, 2012. **322**(1-2): p. 141-7.
31. Lazarov, O. and R.A. Marr, *Neurogenesis and Alzheimer's disease: at the crossroads.* Exp Neurol, 2010. **223**(2): p. 267-81.
32. Bonfanti, L., *A Vascular Perspective on Neurogenesis*, in *Neural Stem Cells: New Perspectives*. 2013, InTech: Croatia. p. 199-239.
33. Abbott, N.J., *Blood-brain barrier structure and function and the challenges for CNS drug delivery.* J Inherit Metab Dis, 2013. **36**(3): p. 437-49.
34. Bicker, J., et al., *Blood-brain barrier models and their relevance for a successful development of CNS drug delivery systems: A review.* Eur J Pharm Biopharm, 2014. **87**(3): p. 409-432.
35. Begley, D.J., *Delivery of therapeutic agents to the central nervous system: the problems and the possibilities.* Pharmacol Ther, 2004. **104**(1): p. 29-45.
36. Zlokovic, B.V., *Neurovascular pathways to neurodegeneration in Alzheimer's disease and other disorders.* Nat Rev Neurosci, 2011. **12**(12): p. 723-38.
37. Bernacki, J., et al., *Physiology and pharmacological role of the blood-brain barrier.* Pharmacol Rep, 2008. **60**(5): p. 600-22.
38. Wallez, Y. and P. Huber, *Endothelial adherens and tight junctions in vascular homeostasis, inflammation and angiogenesis.* Biochim Biophys Acta, 2008.

1778(3): p. 794-809.
39. Alam, M.I., et al., *Strategy for effective brain drug delivery.* Eur J Pharm Sci, 2010. **40**(5): p. 385-403.
40. Park, J.A., et al., *Coordinated interaction of the vascular and nervous systems: from molecule- to cell-based approaches.* Biochem Biophys Res Commun, 2003. **311**(2): p. 247-53.
41. Rocha, S.F. and R.H. Adams, *Molecular differentiation and specialization of vascular beds.* Angiogenesis, 2009. **12**(2): p. 139-47.
42. van Vulpen, M., et al., *Changes in blood-brain barrier permeability induced by radiotherapy: implications for timing of chemotherapy? (Review).* Oncol Rep, 2002. **9**(4): p. 683-8.
43. Brown, R.C., R.D. Egleton, and T.P. Davis, *Mannitol opening of the blood-brain barrier: regional variation in the permeability of sucrose, but not 86Rb+ or albumin.* Brain Res, 2004. **1014**(1-2): p. 221-7.
44. Yilmaz, N., et al., *Activity of mannitol and hypertonic saline therapy on the oxidant and antioxidant system during the acute term after traumatic brain injury in the rats.* Brain Res, 2007. **1164**: p. 132-5.
45. Kang, E.J., et al., *Blood-brain barrier opening to large molecules does not imply blood-brain barrier opening to small ions.* Neurobiol Dis, 2013. **52**: p. 204-18.
46. Radu, M. and J. Chernoff, *An in vivo assay to test blood vessel permeability.* J Vis Exp, 2013(73): p. e50062.
47. Chen, K.B., et al., *Intravenous mannitol does not increase blood-brain barrier permeability to inert dyes in the adult rat forebrain.* Neuroreport, 2013. **24**(6): p. 303-7.
48. Bailey, T.L., et al., *The nature and effects of cortical microvascular pathology in aging and Alzheimer's disease.* Neurol Res, 2004. **26**(5): p. 573-8.
49. Farkas, E. and P.G. Luiten, *Cerebral microvascular pathology in aging and Alzheimer's disease.* Prog Neurobiol, 2001. **64**(6): p. 575-611.
50. de la Torre, J.C., *Alzheimer disease as a vascular disorder: nosological evidence.* Stroke, 2002. **33**(4): p. 1152-62.
51. Bell, R.D. and B.V. Zlokovic, *Neurovascular mechanisms and blood-brain barrier disorder in Alzheimer's disease.* Acta Neuropathol, 2009. **118**(1): p. 103-13.
52. Zlokovic, B.V., *Neurovascular mechanisms of Alzheimer's neurodegeneration.* Trends Neurosci, 2005. **28**(4): p. 202-8.
53. Kalaria, R.N. and P. Hedera, *Differential degeneration of the cerebral microvasculature in Alzheimer's disease.* Neuroreport, 1995. **6**(3): p. 477-80.
54. Grammas, P., M. Yamada, and B. Zlokovic, *The cerebromicrovasculature: a key player in the pathogenesis of Alzheimer's disease.* J Alzheimers Dis, 2002. **4**(3): p. 217-23.
55. Ming, G.L. and H. Song, *Adult neurogenesis in the mammalian central nervous system.* Annu Rev Neurosci, 2005. **28**: p. 223-50.

56. Cajal, S.R., ed. *Estudios Sobre la Degeneratión y Regeneratión Del Sistema Nervioso*. 1913, Madrid: Moya.
57. Altman, J. and G.D. Das, *Autoradiographic and histological evidence of postnatal hippocampal neurogenesis in rats.* J Comp Neurol, 1965. **124**(3): p. 319-35.
58. Taupin, P. and F.H. Gage, *Adult neurogenesis and neural stem cells of the central nervous system in mammals.* J Neurosci Res, 2002. **69**(6): p. 745-9.
59. Colucci-D'Amato, L., V. Bonavita, and U. di Porzio, *The end of the central dogma of neurobiology: stem cells and neurogenesis in adult CNS.* Neurol Sci, 2006. **27**(4): p. 266-70.
60. Luskin, M.B., *Restricted proliferation and migration of postnatally generated neurons derived from the forebrain subventricular zone.* Neuron, 1993. **11**(1): p. 173-89.
61. Kempermann, G., et al., *Milestones of neuronal development in the adult hippocampus.* Trends Neurosci, 2004. **27**(8): p. 447-52.
62. Lois, C. and A. Alvarez-Buylla, *Proliferating subventricular zone cells in the adult mammalian forebrain can differentiate into neurons and glia.* Proc Natl Acad Sci U S A, 1993. **90**(5): p. 2074-7.
63. Kempermann, G., L. Wiskott, and F.H. Gage, *Functional significance of adult neurogenesis.* Curr Opin Neurobiol, 2004. **14**(2): p. 186-91.
64. Ming, G.L. and H. Song, *Adult neurogenesis in the mammalian brain: significant answers and significant questions.* Neuron, 2011. **70**(4): p. 687-702.
65. Schouten, M., et al., *New Neurons in Aging Brains: Molecular Control by Small Non-Coding RNAs.* Front Neurosci, 2012. **6**: p. 25.
66. Kazanis, I., et al., *The neural stem cell microenvironment.* 2008.
67. Herrera, D.G., J.M. Garcia-Verdugo, and A. Alvarez-Buylla, *Adult-derived neural precursors transplanted into multiple regions in the adult brain.* Ann Neurol, 1999. **46**(6): p. 867-77.
68. Palmer, T.D., A.R. Willhoite, and F.H. Gage, *Vascular niche for adult hippocampal neurogenesis.* J Comp Neurol, 2000. **425**(4): p. 479-94.
69. Goldman, S.A. and Z. Chen, *Perivascular instruction of cell genesis and fate in the adult brain.* Nat Neurosci, 2011. **14**(11): p. 1382-9.
70. Nakagomi, N., et al., *Endothelial cells support survival, proliferation, and neuronal differentiation of transplanted adult ischemia-induced neural stem/progenitor cells after cerebral infarction.* Stem Cells, 2009. **27**(9): p. 2185-95.
71. Shen, Q., et al., *Endothelial cells stimulate self-renewal and expand neurogenesis of neural stem cells.* Science, 2004. **304**(5675): p. 1338-40.
72. Gritti, A., et al., *Multipotential stem cells from the adult mouse brain proliferate and self-renew in response to basic fibroblast growth factor.* J Neurosci, 1996. **16**(3): p. 1091-100.
73. Hayashi, T., et al., *Temporal profile of angiogenesis and expression of related*

genes in the brain after ischemia. J Cereb Blood Flow Metab, 2003. **23**(2): p. 166-80.

74. Trejo, J.L., E. Carro, and I. Torres-Aleman, *Circulating insulin-like growth factor I mediates exercise-induced increases in the number of new neurons in the adult hippocampus.* J Neurosci, 2001. **21**(5): p. 1628-34.
75. Rodriguez, J.J. and A. Verkhratsky, *Neurogenesis in Alzheimer's disease.* J Anat, 2011. **219**(1): p. 78-89.
76. Lazarov, O. and R.A. Marr, *Of mice and men: neurogenesis, cognition and Alzheimer's disease.* Front Aging Neurosci, 2013. **5**: p. 43.
77. Mu, Y. and F.H. Gage, *Adult hippocampal neurogenesis and its role in Alzheimer's disease.* Mol Neurodegener, 2011. **6**: p. 85.
78. Jin, K., et al., *Increased hippocampal neurogenesis in Alzheimer's disease.* Proc Natl Acad Sci U S A, 2004. **101**(1): p. 343-7.
79. Li, B., et al., *Failure of neuronal maturation in Alzheimer disease dentate gyrus.* J Neuropathol Exp Neurol, 2008. **67**(1): p. 78-84.
80. Ziabreva, I., et al., *Altered neurogenesis in Alzheimer's disease.* J Psychosom Res, 2006. **61**(3): p. 311-6.
81. Perry, E.K., et al., *Neurogenic abnormalities in Alzheimer's disease differ between stages of neurogenesis and are partly related to cholinergic pathology.* Neurobiol Dis, 2012. **47**(2): p. 155-62.
82. Chen, Q., et al., *Adult neurogenesis is functionally associated with AD-like neurodegeneration.* Neurobiol Dis, 2008. **29**(2): p. 316-26.
83. Rodriguez, J.J., et al., *Impaired adult neurogenesis in the dentate gyrus of a triple transgenic mouse model of Alzheimer's disease.* PLoS One, 2008. **3**(8): p. e2935.
84. Kaneko, N. and K. Sawamoto, *Adult neurogenesis and its alteration under pathological conditions.* Neurosci Res, 2009. **63**(3): p. 155-64.
85. Demars, M., et al., *Impaired neurogenesis is an early event in the etiology of familial Alzheimer's disease in transgenic mice.* J Neurosci Res, 2010. **88**(10): p. 2103-17.
86. Jin, K., et al., *Alzheimer's disease drugs promote neurogenesis.* Brain Res, 2006. **1085**(1): p. 183-8.
87. Varela-Nallar, L., et al., *Adult hippocampal neurogenesis in aging and Alzheimer's disease.* Birth Defects Res C Embryo Today, 2010. **90**(4): p. 284-96.
88. Joshi, S., et al., *Inconsistent blood brain barrier disruption by intraarterial mannitol in rabbits: implications for chemotherapy.* J Neurooncol, 2011. **104**(1): p. 11-9.
89. Schindelin, J., et al., *Fiji: an open-source platform for biological-image analysis.* Nat Methods, 2012. **9**(7): p. 676-82.
90. Longair, M.H., D.A. Baker, and J.D. Armstrong, *Simple Neurite Tracer: open source software for reconstruction, visualization and analysis of neuronal*

processes. Bioinformatics, 2011. **27**(17): p. 2453-4.
91. Bolte, S. and F.P. Cordelières, *A guided tour into subcellular colocalization analysis in light microscopy.* Journal of Microscopy, 2006. **224**(3): p. 213–232.
92. Arganda-Carreras, I., et al., *3D reconstruction of histological sections: Application to mammary gland tissue.* Microsc Res Tech, 2010. **73**(11): p. 1019-29.
93. Andersen, K., B.B. Andersen, and B. Pakkenberg, *Stereological quantification of the cerebellum in patients with Alzheimer's disease.* Neurobiology of Aging, 2012(33): p. 197.e11-197.e20.
94. Encinas, J.M., et al., *Division-coupled astrocytic differentiation and age-related depletion of neural stem cells in the adult hippocampus.* Cell Stem Cell, 2011. **8**(5): p. 566-79.
95. Do, T.M., et al., *Altered cerebral vascular volumes and solute transport at the blood-brain barriers of two transgenic mouse models of Alzheimer's disease.* Neuropharmacology, 2014. **81**: p. 311-7.
96. Miao, J., et al., *Cerebral microvascular amyloid beta protein deposition induces vascular degeneration and neuroinflammation in transgenic mice expressing human vasculotropic mutant amyloid beta precursor protein.* Am J Pathol, 2005. **167**(2): p. 505-15.
97. Attems, J., et al., *Capillary CAA and perivascular Abeta-deposition: two distinct features of Alzheimer's disease pathology.* J Neurol Sci, 2010. **299**(1-2): p. 155-62.
98. Austin, S.A., A.V. Santhanam, and Z.S. Katusic, *Endothelial nitric oxide modulates expression and processing of amyloid precursor protein.* Circ Res, 2010. **107**(12): p. 1498-502.
99. Rajadas, J., et al., *Enhanced Abeta(1-40) production in endothelial cells stimulated with fibrillar Abeta(1-42).* PLoS One, 2013. **8**(3): p. e58194.
100. Fonseca, A.C., et al., *Activation of the endoplasmic reticulum stress response by the amyloid-beta 1-40 peptide in brain endothelial cells.* Biochim Biophys Acta, 2013. **1832**(12): p. 2191-203.
101. Fonseca, A.C., et al., *Amyloid-Beta Disrupts Calcium and Redox Homeostasis in Brain Endothelial Cells.* Mol Neurobiol, 2014.
102. Fonseca, A.C., et al., *Loss of proteostasis induced by amyloid beta peptide in brain endothelial cells.* Biochim Biophys Acta, 2014. **1843**(6): p. 1150-61.
103. Hardy, J. and D.J. Selkoe, *The amyloid hypothesis of Alzheimer's disease: progress and problems on the road to therapeutics.* Science, 2002. **297**(5580): p. 353-6.
104. Zlokovic, B.V., *The blood-brain barrier in health and chronic neurodegenerative disorders.* Neuron, 2008. **57**(2): p. 178-201.
105. Merlini, M., et al., *Vascular beta-amyloid and early astrocyte alterations impair cerebrovascular function and cerebral metabolism in transgenic arcAbeta mice.*

Acta Neuropathol, 2011. **122**(3): p. 293-311.
106. Jaworski, T., et al., *Dendritic degeneration, neurovascular defects, and inflammation precede neuronal loss in a mouse model for tau-mediated neurodegeneration.* Am J Pathol, 2011. **179**(4): p. 2001-15.
107. Marques, F., et al., *Blood-brain-barriers in aging and in Alzheimer's disease.* Mol Neurodegener, 2013. **8**: p. 38.
108. Abrous, D.N., M. Koehl, and M. Le Moal, *Adult neurogenesis: from precursors to network and physiology.* Physiol Rev, 2005. **85**(2): p. 523-69.
109. Donovan, M.H., et al., *Decreased adult hippocampal neurogenesis in the PDAPP mouse model of Alzheimer's disease.* J Comp Neurol, 2006. **495**(1): p. 70-83.
110. Hamilton, L.K., et al., *Widespread deficits in adult neurogenesis precede plaque and tangle formation in the 3xTg mouse model of Alzheimer's disease.* Eur J Neurosci, 2010. **32**(6): p. 905-20.
111. Valero, J., et al., *Short-term environmental enrichment rescues adult neurogenesis and memory deficits in APP(Sw,Ind) transgenic mice.* PLoS One, 2011. **6**(2): p. e16832.
112. Katsimpardi, L., et al., *Vascular and neurogenic rejuvenation of the aging mouse brain by young systemic factors.* Science, 2014. **344**(6184): p. 630-4.